

THE UNIVERSITY OF MELBOURNE

DOCTORAL THESIS

The Coupling Time for the Ising Heat-Bath Dynamics & Efficient Optimization for Statistical Inference

Author:

Timothy HYNDMAN

Supervisors:

Prof. Peter TAYLOR

Prof. Aurore DELAIGLE

Assoc. Prof. Tim GARONI

*Submitted in total fulfilment of the requirements
of the degree of Doctor of Philosophy*

Operations Research
School of Mathematics and Statistics

August 2018

THE UNIVERSITY OF MELBOURNE

Abstract

Faculty of Science

School of Mathematics and Statistics

Doctor of Philosophy

**The Coupling Time for the Ising Heat-Bath Dynamics & Efficient
Optimization for Statistical Inference**

by Timothy HYNDMAN

The title page must be followed by an abstract of 300–500 words in English. The Thesis Abstract is written here (and usually kept to just this page). The page is kept centered vertically so can expand into the blank space above the title too.

Declaration of Authorship

This is to certify that:

1. the thesis comprises only my original work towards the PhD except where indicated in the Preface,
2. due acknowledgement has been made in the text to all other material used,
3. the thesis is fewer than 100 000 words in length, exclusive of tables, maps, bibliographies and appendices.

Signed:

Date:

Preface

If applicable, a Preface page includes a statement of:

- Work carried out in collaboration indicating the nature and proportion of the contribution of others and in general terms the portions of the work which the candidate claims as original
- Work submitted for other qualifications
- Work carried out prior to PhD candidature enrolment
- any third party editorial assistance, either paid or voluntary (as limited to the Editing of Research Theses by Professional Editors guidelines) and/or
- Where a substantially unchanged multi-author paper is included in the thesis a statement prepared by the candidate explaining the contributions of all involved. A signed copy by all authors must be included with the submission form.

“Thanks to my solid academic training, today I can write hundreds of words on virtually any topic without possessing a shred of information, which is how I got a good job in journalism.”

Dave Barry

Acknowledgements

The acknowledgements and the people to thank go here, don't forget to include your project advisor...

Contents

Abstract	i
Declaration of Authorship	ii
Preface	iii
Acknowledgements	v
Contents	vi
List of Figures	ix
1 Introduction to this Thesis	1
I The Coupling Time for the Ising Heat-Bath Dynamics	2
2 Introduction	3
2.1 The Ising Model	3
2.1.1 The Phase Transition	4
2.2 Coupling from the Past	5
2.2.1 Ising heat-bath Glauber dynamics	5
2.2.2 The Coupling Time	6
2.2.3 Equivalence of Discrete and Continuous Coupling Time	7
2.2.4 Summary of CFTP	11
2.3 Information percolation	12
2.3.1 Information percolation and cutoff for the stochastic Ising model .	12
2.3.2 The framework	13
2.3.2.1 The update sequence	14
2.3.2.2 The update support function	14
2.3.2.3 Oblivious updates	16
3 The Coupling Time on the Cycle	19
3.1 Information percolation on the cycle	19
3.1.1 Update histories on the cycle	20

3.2	Compound Poisson Approximation	21
3.3	Proof of Theorem 3.1	23
3.3.1	Additional Lemmas	26
4	The Coupling Time on Vertex Transitive Graphs	30
4.1	Information Percolation in higher dimensions	30
4.1.1	Magnetization	31
4.2	Setup	32
4.3	Proof of Theorem 4.1	33
4.3.1	Additional Lemmas	35
5	Conclusion	40
II	Efficient Optimization for Statistical Inference	41
6	Introduction	42
7	Maximum Likelihood Location Mixtures	43
7.1	Introduction	43
7.1.1	Definitions	43
7.1.2	Flag graphs	44
7.1.3	Motivating Example	45
7.2	Results for $n = 2$	45
7.2.1	Things that are referenced	45
7.2.2	The likelihood curve	45
7.2.2.1	An example	46
7.2.3	The likelihood curve for $n = 2$	47
7.3	Results for general n	51
7.3.1	Directional Derivative	51
7.3.2	Normal Constraints	51
7.3.2.1	Treating \mathbf{x} as random	52
7.3.3	Properties of Γ	53
7.3.4	Bounding C_m	54
7.3.5	A particular class of optimization problem	54
7.3.6	Derive Constraints again	55
7.4	General Results	55
7.4.1	All points separated by α	55
7.4.2	Discussion about what we hope to achieve	56
8	Deconvolution	57
8.1	Introduction	57
8.1.1	Optimization problem	58
8.1.2	Kernel Smoothing	58
8.2	Examples and Relation to Mixture Phenomenon	58
8.3	R Package	58

Bibliography

59

List of Figures

2.1	Typical appearance of the update histories for two vertices on the cycle	14
2.2	A naive construction of the update history of i	16
2.3	The update sequence for a section of the cycle and the corresponding update history from vertex i	18
2.4	A non-oblivious update that shrinks the size of the update history	18
7.1	K as a function of x_2 and x_3 (with $x_1 = 0$) for a normal component density with unit variance.	44
7.2	The blue density is f_θ for $\theta = 1, 2, 3$. Each value of θ contributes a point to Γ whose coordinates are given by $(f_\theta(X_1), f_\theta(X_2))$ (represented by the red circles). As we increase θ from $-\infty$ to ∞ we trace out more of Γ (shown above).	46
7.3	In (a), the boundary of $\text{Conv}(\Gamma)$ is shown as a dashed black line, Γ is the white curve, the heat map shows the objective function (likelihood increases from blue to yellow) and the yellow point is the maximizing point which can be written as the convex combination of the two magenta points. These two magenta points correspond to the two probability masses in the maximizing mixing distribution (b).	47
7.4	The curve $\Gamma_{\mathbf{x}}$ for three different \mathbf{x} along with the boundary of $\text{Conv}(\Gamma_{\mathbf{x}})$. The objective function from (7.9) is represented as a heat map. The optimal point $\hat{\mathbf{u}}$ is shown in yellow, and where applicable, the points $\gamma(\theta_j)$ that make up $\hat{\mathbf{u}}$ (as in (7.8)) are shown in magenta.	48

For/Dedicated to/To my...

Chapter 1

Introduction to this Thesis

Initially, this thesis was intended to be made up entirely of the contents of Part [II](#), along with what we hoped would be several significant further contributions to the study. However, the practicalities of a deadline, along with the challenging nature of the research, meant that the decision was made to augment this thesis with an essentially separate section of study. This is what makes up Part [I](#).

The reader should view these two parts as standalone topics, to be read independently. However, they are not without any commonality. Both are within the realm of stochastic mathematics, Part [I](#) being a study of a random variable constructed from a stochastic process, and Part [II](#) being a study of probability distributions that maximize certain statistical objective functions.

Part I

The Coupling Time for the Ising Heat-Bath Dynamics

Chapter 2

Introduction

2.1 The Ising Model

The Ising model is named after Ernst Ising who studied it in his 1924 thesis [1] under the supervision of Wilhelm Lenz who invented the model [2]. It was originally motivated by the phenomenon of ferromagnetism but it has since been re-interpreted to apply to numerous other situations in both physics and other fields ¹.

The Ising model has enjoyed a prominent position in the statistical physics literature. This is largely due to the existence of a phase transition, a sharp transition in the large scale behaviour of the model as a parameter moves past a critical value. The transition was first shown to exist by Rudolph Peierls [4] in what was the first proof of the existence of a phase transition for any model in statistical mechanics. Additionally, the Ising model is both relatively simple, and also mathematically tractable in some non-trivial cases [5]. These qualities are rare among models with a phase transition and so the Ising model has become somewhat of a staple for both studying phase transitions and testing new statistical mechanics techniques.

The model is a probability distribution on spin configurations - assignments of $+1$ and -1 spins to each vertex in a finite graph $G = (V, E)$. The set of all possible configurations is

$$\Omega = \{-1, +1\}^V \tag{2.1}$$

and for a particular configuration, $\sigma \in \Omega$, we refer to the spin of a particular vertex $i \in V$ with $\sigma[i]$. Each configuration has an associated energy, given by

$$H_{G,\beta,h}(\sigma) = -\beta \sum_{ij \in E} \sigma[i]\sigma[j] - h \sum_{i \in V} \sigma[i] \tag{2.2}$$

¹See [3, notes of Section 1.4.2] for a list of references concerning this.

where $\beta \in [0, \infty)$ is the inverse temperature, and $h \in \mathbb{R}$ is the magnetic field.

The Gibbs measure is the distribution on Ω that characterises the Ising model and it is defined by

$$\pi_{G,\beta,h}(\sigma) \propto \exp(-H_{G,\beta,h}(\sigma)). \quad (2.3)$$

In everything that follows, we will be concerned only with the zero-field ($h = 0$) Ising model. This gives us the slightly simpler form for the Gibbs measure,

$$\pi_{G,\beta}(\sigma) \propto \exp\left(\beta \sum_{ij \in E} \sigma[i]\sigma[j]\right), \quad \sigma \in \{-1, 1\}^V. \quad (2.4)$$

2.1.1 The Phase Transition

An in depth study of the Ising phase transition and its associated critical temperature will not be needed for this work. However, we will still wish to refer to it occasionally and so here we give a workable description of the phase transition on lattices.

Consider the Gibbs measure with zero-field (2.4) in the limits $\beta \downarrow 0$ and $\beta \uparrow \infty$. It is easy to see that in the former limit, the measure is uniform across all configurations and in the latter limit, the measure assigns all weight to the constant configurations $\sigma^- = (-1, -1, \dots, -1)$ and $\sigma^+ = (+1, +1, \dots, +1)$. This leads to the following overly simplistic description of the phase transition. It is the change in distribution that occurs as we increase the temperature; from distributions concentrated on states whose spins mostly agree, to distributions producing states which have roughly equal numbers of plus and minus spins.

To be slightly more concrete we define quantities called the magnetization and magnetization density. The *magnetization* on a volume $\Lambda \subseteq V$ is defined as

$$M_\Lambda(\sigma) = \sum_{i \in \Lambda} \sigma[i]. \quad (2.5)$$

Normalizing this gives the *magnetization density*, $M_\Lambda(\sigma)/|\Lambda|$. On the d -dimensional torus with side length L , $G(L) = (\mathbb{Z}/L\mathbb{Z})^d$, the quantity

$$L(\beta) = \lim_{L \rightarrow \infty} \mathbb{E}_\beta \left| \frac{M_{G(L)}(\sigma)}{|G(L)|} \right| \quad (2.6)$$

depends on the inverse temperature β . When $d = 1$, $L(\beta) = 0$ for any β and there is no phase transition. However, when $d > 1$, there exists some critical $\beta_c(d)$ such that $L(\beta) = 0$ for $\beta < \beta_c(d)$ and $L(\beta) > 0$ for $\beta > \beta_c(d)$ [3]. This $\beta_c(d)$ is the critical inverse temperature at which we observe a phase transition.

2.2 Coupling from the Past

One of the primary concerns regarding the Ising model is how to efficiently sample from the Gibbs measure. Calculating the normalizing constant for (2.4), known as the partition function, is a #P-complete problem [6]. As such a direct approach to sampling is computationally intractable and so other methods must be employed instead. One such method is Markov Chain Monte Carlo (MCMC). This involves constructing a Markov chain whose states are elements of Ω and whose stationary distribution is given by (2.4). One can then obtain a sample by running this Markov chain for long enough that the output has distribution sufficiently close to (2.4). One difficulty in using MCMC is that, initially, one does not know how long to run the chain for. In principal, bounds on this time can be achieved, but in practise, proving these bounds can be very challenging.

An alternative to MCMC was introduced by Propp and Wilson called Coupling from the Past (CFTP) [7]. Unlike MCMC, CFTP not only has an automatically determined running time, but it has the additional advantage of outputting exact samples from the stationary distribution. This does not come without a cost - CFTP has a random running time. Therefore, a key question towards evaluating the effectiveness of CFTP is understanding the distribution of its running time, that is, the *coupling time*.

In Chapters 3 and 4, we will investigate the coupling time for the Ising heat-bath Glauber dynamics, both on the cycle, at any temperature, in Chapter 3, and on any vertex transitive graph, at sufficiently high temperatures, in Chapter 4. Our main result in each chapter will be proving that, when appropriately scaled, the coupling time essentially converges to a Gumbel distribution as the size of the graph increases.

2.2.1 Ising heat-bath Glauber dynamics

The continuous-time heat-bath Glauber dynamics for the Ising model is a Markov chain whose states are elements of Ω and whose stationary distribution is given by (2.4). For a given graph $G = (V, E)$, and a given inverse temperature, β , we can describe the dynamics as follows.

Initialize every vertex in V with a spin (for example, we could start in the all-plus configuration). To each vertex in V we give an i.i.d. rate-one Poisson clock. Define the probability

$$p_i(\sigma) = \frac{e^{\beta S_i(\sigma)}}{e^{\beta S_i(\sigma)} + e^{-\beta S_i(\sigma)}} \quad (2.7)$$

where

$$S_i(\sigma) = \sum_{j \sim i} \sigma[j] \quad (2.8)$$

is the sum of the spins of the neighbours of i , and $j \sim i$ denotes that j is connected to i with some edge $ij \in E$. Let σ_t denote the spin configuration at time t . When the clock of vertex i rings at some time t , we update $\sigma_t[i]$ to $+1$ with probability $p_i(\sigma_t)$, and to -1 otherwise.

2.2.2 The Coupling Time

We now describe the two coupled chains from which we define the coupling time of the Ising heat-bath Glauber dynamics. In order to do this, it will prove convenient to use a random mapping representation for the jump process. This will also help us outline an implementation of CFTP for our coupling.

Define $f : \Omega \times V \times [0, 1] \mapsto \Omega$ via $f(\sigma, i, u) = \sigma'$ where $\sigma'[j] = \sigma[j]$ for $j \neq i$ and

$$\sigma'[i] = \begin{cases} 1, & u \leq p_i(\sigma), \\ -1, & u > p_i(\sigma). \end{cases} \quad (2.9)$$

Let \mathcal{V} and U be independent, with \mathcal{V} uniform on V and U uniform on $[0, 1]$. Then, updating our chain at rate $n = |V|$, and performing updates from σ to σ' according to $\sigma' = f(\sigma, \mathcal{V}, U)$, we recover the dynamics described in Section 2.2.1.

We also note that f is monotonic, in the following sense. We define a partial ordering on Ω by writing that $\sigma \preceq \omega$ if $\sigma, \omega \in \Omega$ are such that $\sigma[i] \leq \omega[i]$ for all $i \in V$ (and similarly for $\sigma \succeq \omega$). Then for any fixed $i \in V$ and $u \in [0, 1]$, if $\sigma \preceq \omega$ then $f(\sigma, i, u) \preceq f(\omega, i, u)$.

Let $(\mathcal{V}_k, U_k)_{k \geq 1}$ be an i.i.d. sequence of copies of (\mathcal{V}, U) . Define top and bottom chains, $(\mathcal{T}_t)_{t \geq 0}$ and $(\mathcal{B}_t)_{t \geq 0}$, with initial states

$$\mathcal{T}_0 = (1, 1, \dots, 1) \quad (2.10)$$

$$\mathcal{B}_0 = (-1, -1, \dots, -1) \quad (2.11)$$

that update together at rate n . On the k th update at time t_k , update \mathcal{T}_{t_k} to $f(\mathcal{T}_{t_k}, \mathcal{V}_k, U_k)$ and update \mathcal{B}_{t_k} to $f(\mathcal{B}_{t_k}, \mathcal{V}_k, U_k)$.

We call the coupled process, $(\mathcal{B}_t, \mathcal{T}_t)_{t \geq 0}$, *the Ising heat-bath coupling*. From the monotonicity of f , $\mathcal{T}_t \succeq \mathcal{B}_t$, for all $t \geq 0$.

A more descriptive explanation of the coupling is that the top and bottom chains share the same rate-one Poisson clocks at each vertex, and upon updating that vertex, we share

the same uniform random variable U between the two chains to determine whether to update to a plus or minus according to (2.9).

The *coupling time* of the Ising heat-bath process is the random variable

$$T = \inf \{t : \mathcal{T}_t = \mathcal{B}_t\}. \quad (2.12)$$

This is the main object of interest for our analysis. Note that the coupling time is not just a property of the Ising heat-bath process, but also of the coupling we have chosen. In Section 3.1 we will make a change to the coupling we use to make the analysis easier. Some care will need to be taken to verify that the coupling time is not affected by this change.

2.2.3 Equivalence of Discrete and Continuous Coupling Time

So far we have stated that the running time of CFTP has the same distribution as the coupling time. In fact, we have glossed over one important detail. Namely, CFTP is exclusively run in discrete time, and our coupling time is defined by the continuous time dynamics. Therefore, for our motivation to be reasonable, we would like to show some sort of equivalence between the distributions of the discrete and continuous coupling times. We do this via Claim 2.2 which first requires the following Lemma.

Lemma 2.1. *Let $T(k)$ be the sum of k i.i.d. rate λ exponentials. For all $0 < \epsilon < 1$,*

$$\mathbb{P} \left(\left| \frac{T(k)\lambda}{k} - 1 \right| \geq \epsilon \right) \leq 2 \exp(-k\epsilon^2/4) \quad (2.13)$$

Proof.

$$\mathbb{P} \left(\left| \frac{T(k)\lambda}{k} - 1 \right| \geq \epsilon \right) = \mathbb{P} \left(\frac{T(k)\lambda}{k} \leq 1 - \epsilon \right) + \mathbb{P} \left(\frac{T(k)\lambda}{k} \geq 1 + \epsilon \right) \quad (2.14)$$

Since $T(k)$ is the sum of k i.i.d. rate λ exponentials, its moment generating function is

$$M_k(t) = \left(\frac{\lambda}{\lambda - t} \right)^k, \quad t < \lambda. \quad (2.15)$$

Using a Chernoff bound, for all $0 < t < \lambda$,

$$\mathbb{P} \left(\frac{T(k)\lambda}{k} \geq 1 + \epsilon \right) = \mathbb{P} \left(T(k) \geq \frac{k}{\lambda}(1 + \epsilon) \right) \quad (2.16)$$

$$\leq \left(\frac{\lambda}{\lambda - t} \right)^k \exp \left(-\frac{tk}{\lambda}(1 + \epsilon) \right) \quad (2.17)$$

$$= \exp(k(\ln(\lambda/(\lambda - t)) - t(1 + \epsilon)/\lambda)). \quad (2.18)$$

Taking $t = \lambda - \lambda/(1 + \epsilon)$,

$$\mathbb{P}\left(\frac{T(k)\lambda}{k} \geq 1 + \epsilon\right) \leq \exp(k(\log(1 + \epsilon) - \epsilon)). \quad (2.19)$$

Similarly, for all $t < 0$,

$$\mathbb{P}\left(\frac{T(k)\lambda}{k} \leq 1 - \epsilon\right) = \mathbb{P}\left(T(k) \leq \frac{k}{\lambda}(1 - \epsilon)\right) \quad (2.20)$$

$$\leq \left(\frac{\lambda}{\lambda - t}\right)^k \exp\left(-\frac{tk}{\lambda}(1 - \epsilon)\right) \quad (2.21)$$

$$= \exp(k(\ln(\lambda/(\lambda - t)) - t(1 - \epsilon)/\lambda)). \quad (2.22)$$

Taking $t = \lambda - \lambda/(1 - \epsilon)$,

$$\mathbb{P}\left(\frac{T(k)\lambda}{k} \leq 1 - \epsilon\right) \leq \exp(k(\log(1 - \epsilon) + \epsilon)). \quad (2.23)$$

Overall,

$$\mathbb{P}\left(\left|\frac{T(k)\lambda}{k} - 1\right| \geq \epsilon\right) \leq \exp(k(\log(1 - \epsilon) + \epsilon)) + \exp(k(\log(1 + \epsilon) - \epsilon)) \quad (2.24)$$

$$\leq 2 \exp(k(\log(1 + \epsilon) - \epsilon)) \quad (2.25)$$

$$\leq 2 \exp(-k\epsilon^2/4) \quad (2.26)$$

for $0 < \epsilon < 1$. □

Claim 2.2. Let $(N_n)_{n \in \mathbb{N}}$ be a sequence of positive random integers, and $(m_n)_{n \in \mathbb{N}}$ be a non-decreasing sequence of integers such that $N_n \geq m_n$ for all n and $\lim_{n \rightarrow \infty} m_n = \infty$. Define $T(n)$ be the random time it takes for a rate λ Poisson clock to go off n times (this is the time it takes for n updates to occur in a continuous-time Markov Chain).

Let a_n and b_n be positive deterministic sequences such that $b_n/a_n \rightarrow \infty$ and

$$m_n \frac{a_n^2}{64b_n^2} - \log \frac{b_n^2}{a_n^2} \rightarrow \infty. \quad (2.27)$$

Define

$$Y_n = \frac{T(N_n) - b_n}{a_n} \quad (2.28)$$

and

$$Z_n = \frac{N_n - \lambda b_n}{\lambda a_n}. \quad (2.29)$$

Let X be a random variable which doesn't place any mass at infinity. Then $Y_n \xrightarrow{d} X$ if and only if $Z_n \xrightarrow{d} X$.

Proof. In order to prove either direction, it is sufficient to show that for any $\epsilon > 0$,

$$\lim_{n \rightarrow \infty} \mathbb{P}(|Y_n - Z_n| > \epsilon) = 0. \quad (2.30)$$

First note that

$$|Y_n - Z_n| = \left| \frac{T(N_n) - b_n}{a_n} - \frac{N_n - \lambda b_n}{\lambda a_n} \right| \quad (2.31)$$

$$= \left| \frac{T(N_n)}{a_n} - \frac{N_n}{\lambda a_n} \right| \quad (2.32)$$

$$= \left| \frac{T(N_n)\lambda}{N_n} - 1 \right| \frac{N_n}{\lambda a_n}. \quad (2.33)$$

So for any $\epsilon > 0$

$$\mathbb{P}(|Y_n - Z_n| > \epsilon) \leq \mathbb{P}\left(\left|\frac{T(N_n)\lambda}{N_n} - 1\right| > \epsilon \frac{a_n}{4b_n}\right) + \mathbb{P}\left(\frac{N_n}{\lambda a_n} > \frac{4b_n}{a_n}\right). \quad (2.34)$$

We will show that both of the terms on the right hand side vanish as $n \rightarrow \infty$. We start with the first of these.

Since $N_n \geq m_n$,

$$\mathbb{P}\left(\left|\frac{T(N_n)\lambda}{N_n} - 1\right| > \epsilon \frac{a_n}{4b_n}\right) \leq \mathbb{P}\left(\sup_{k \geq m_n} \left|\frac{T(k)\lambda}{k} - 1\right| > \epsilon \frac{a_n}{4b_n}\right) \quad (2.35)$$

$$= \mathbb{P}\left(\bigcup_{k \geq m_n} \left\{\left|\frac{T(k)\lambda}{k} - 1\right| > \epsilon \frac{a_n}{4b_n}\right\}\right) \quad (2.36)$$

$$\leq \sum_{k=m_n}^{\infty} \mathbb{P}\left(\left|\frac{T(k)\lambda}{k} - 1\right| > \epsilon \frac{a_n}{4b_n}\right). \quad (2.37)$$

To apply Lemma 2.1, we need that $\epsilon a_n/(4b_n) < 1$. However, since $a_n/b_n \rightarrow 0$, we can ensure this holds by taking n large enough. In fact, in what follows we will assume n is large enough that $a_n < b_n$. Continuing,

$$\sum_{k=m_n}^{\infty} \mathbb{P}\left(\left|\frac{T(k)\lambda}{k} - 1\right| > \epsilon \frac{a_n}{4b_n}\right) \leq 2 \sum_{k=m_n}^{\infty} \exp\left(-k \frac{a_n^2}{64b_n^2}\right) \quad (2.38)$$

$$= 2 \frac{\exp(-a_n^2(m_n - 1)/(64b_n^2))}{\exp(a_n^2/(64b_n^2)) - 1}. \quad (2.39)$$

Since $x \leq \exp(x) - 1$ for $0 \leq x \leq 1$,

$$2 \frac{\exp(-a_n^2(m_n - 1)/(64b_n^2))}{\exp(a_n^2/(64b_n^2)) - 1} \leq \frac{128b_n^2}{a_n^2} \exp(-a_n^2(m_n - 1)/(64b_n^2)) \quad (2.40)$$

$$\leq 256 \frac{b_n^2}{a_n^2} \exp(-m_n a_n^2/(64b_n^2)) \quad (2.41)$$

where we have again used that $a_n < b_n$. By (2.27), this goes to zero as $n \rightarrow \infty$.

To bound the second term in (2.34), we will treat the two directions of the proof separately. Firstly, assume that $Z_n \xrightarrow{d} X$. Then note that

$$\mathbb{P}\left(\frac{N_n}{\lambda a_n} > \frac{4b_n}{a_n}\right) = \mathbb{P}\left(Z_n > 3\frac{b_n}{a_n}\right) \quad (2.42)$$

and since $b_n/a_n \rightarrow \infty$, and Z_n converges to a distribution which places no mass at ∞ ,

$$\lim_{n \rightarrow \infty} \mathbb{P}\left(\frac{N_n}{\lambda a_n} > \frac{4b_n}{a_n}\right) = 0. \quad (2.43)$$

Now assume that $Y_n \xrightarrow{d} X$. Note that if $T(N_n)/a_n < \epsilon/2$ and $|T(N_n)\lambda/N_n - 1| < 1/2$, then $N_n/(\lambda a_n) < \epsilon$. So

$$\mathbb{P}\left(\frac{N_n}{\lambda a_n} > \frac{4b_n}{a_n}\right) \leq \mathbb{P}\left(\frac{T(N_n)}{a_n} < \frac{2b_n}{a_n}\right) + \mathbb{P}\left(\left|\frac{T(N_n)\lambda}{N_n} - 1\right| > \frac{1}{2}\right) \quad (2.44)$$

$$= \mathbb{P}\left(Y_n < \frac{b_n}{a_n}\right) + \mathbb{P}\left(\left|\frac{T(N_n)\lambda}{N_n} - 1\right| > \frac{1}{2}\right). \quad (2.45)$$

As above, since $a_n/b_n \rightarrow \infty$, and Y_n converges to a distribution which places no mass at ∞ , the first term vanishes in the limit. The second disappears since

$$\mathbb{P}\left(\left|\frac{T(N_n)\lambda}{N_n} - 1\right| > \frac{1}{2}\right) \leq \mathbb{P}\left(\left|\frac{T(N_n)\lambda}{N_n} - 1\right| > \epsilon \frac{a_n}{4b_n}\right) \quad (2.46)$$

for large enough n .

□

Remark 2.3. We apply Claim 2.2 to the coupling time of the Glauber heat-bath dynamics in the following way. Take N_n to be the discrete coupling time on a graph of size n . The continuous time coupling time is given by $T(N_n)$. Note that $N_n \geq m_n = n$ since each vertex must be updated at least once for coupling to occur. Finally Theorems 3.1 and 4.1 establish the limiting distribution of the continuous-time coupling time using scaling and shifting sequences a_n and b_n whose ratio is

$$\frac{b_n}{a_n} = \log n \quad (2.47)$$

and thus (2.27) is satisfied. This means that, appropriately scaled, the discrete-time coupling time has the same limiting distribution as the continuous-time coupling time.

2.2.4 Summary of CFTP

We are now in a position to give a brief summary of the CFTP method, as it applies to the Ising heat-bath coupling. It should be noted that we include this summary of CFTP for completeness. None of the details regarding the implementation of CFTP are required outside of this section. It serves only as motivation for the study of the coupling time.

Let $f : \Omega \times V \times [0, 1] \mapsto \Omega$ and (\mathcal{V}, U) be as defined in Section 2.2.2. Let (\mathcal{V}_k, U_k) be an i.i.d. sequence of copies of (\mathcal{V}, U) and define

$$f_{-k} = f(\cdot, \mathcal{V}_k, U_k). \quad (2.48)$$

We construct the composition

$$F_{-k} = f_0 \circ f_1 \circ \cdots \circ f_{k-1} \quad (2.49)$$

and define the *backwards coupling time* to be

$$T_{\text{BACK}} = \min\{k \in \mathbb{N} : F_{-k}(\mathcal{B}_0) = F_{-k}(\mathcal{T}_0)\}. \quad (2.50)$$

The state $F_{-T_{\text{BACK}}}(\mathcal{B}_0) = F_{-T_{\text{BACK}}}(\mathcal{T}_0)$ is the output of the CFTP algorithm, and was shown by Propp and Wilson [7] to be an exact sample from the chain's stationary distribution. To see why this is so, observe that by the monotonicity of f , if $F_{-k}(\mathcal{B}_0) = F_{-k}(\mathcal{T}_0)$, then $F_{-k}(\sigma) = F_{-k}(\mathcal{B}_0)$ for any $\sigma \in \Omega$. If we let σ_π be a random sample from the stationary distribution π , then $F_{-k}(\mathcal{B}_0) = F_{-k}(\mathcal{T}_0) = F_{-k}(\sigma_\pi)$ must also have distribution π , which in our case is given by (2.4).

If we reverse the composition to construct

$$F_k = f_k \circ f_{k-1} \circ \cdots \circ f_1 \quad (2.51)$$

we can define the usual discrete time coupling time as

$$T_{\text{DIS}} = \min\{k \in \mathbb{N} : F_k(\mathcal{B}_0) = F_k(\mathcal{T}_0)\}. \quad (2.52)$$

The forwards coupling time, T_{DIS} , has the same distribution as the backwards coupling time, T_{BACK} , although in general, $F_{T_{\text{DIS}}}(\mathcal{B}_0) = F_{T_{\text{DIS}}}(\mathcal{T}_0)$ does not have distribution (2.4).

In practise, one runs the CFTP algorithm by starting both the top and bottom chains from some point in the past to time zero. This is repeated for increasingly more distant times in the past until both chains agree at time 0. The sequence of times at which one restarts this process need not be $-1, -2, -3, \dots$, rather, any monotonic natural sequence a_1, a_2, \dots can be used. See [8], [9], and [10] for further discussion.

2.3 Information percolation

A cornerstone to the proofs contained in Chapters 3 and 4 is the framework of information percolation, first introduced by Lubetzky and Sly in 2016 [11]. In this paper, Lubetzky and Sly managed to achieve much sharper results, in much more generality, regarding the mixing time for the Glauber dynamics for the Ising model than had been achieved before. In this section we provide a brief summary of their paper before laying out the basic framework, in the context of the Ising heat-bath dynamics, that will be required for Chapters 3 and 4.

2.3.1 Information percolation and cutoff for the stochastic Ising model

In order to define cutoff, the central phenomenon of study in Lubetzky and Sly's 2016 paper titled, 'Information percolation and cutoff for the stochastic Ising model', we first have to define the total-variation mixing time. Given a parameter ϵ , a Markov Chain Y_t has mixing time

$$t_{\text{MIX}}(\epsilon) = \inf \left\{ t : \max_{x_0 \in \Omega} \|\mathbb{P}(X_t \in \cdot | X_0 = x_0) - \pi\|_{\text{TV}} \leq \epsilon \right\} \quad (2.53)$$

where the total variation distance $\|\nu_1 - \nu_2\|_{\text{TV}}$ is defined as

$$\max_{A \in \Omega} |\nu_1(A) - \nu_2(A)| = \frac{1}{2} \sum_{\sigma \in \Omega} |\nu_1(\sigma) - \nu_2(\sigma)|. \quad (2.54)$$

A family of Markov chains (Y_t) indexed by n is said to exhibit cutoff if

$$t_{\text{MIX}}(\epsilon) = (1 + o(1))t_{\text{MIX}}(\epsilon'), \quad (2.55)$$

for any fixed $0 < \epsilon, \epsilon' < 1$. A *cutoff window* is a sequence w_n where

$$t_{\text{MIX}}(\epsilon) = t_{\text{MIX}}(1 - \epsilon) + \mathcal{O}(w_n) \quad (2.56)$$

for any $0 < \epsilon < 1$.

Historically, proving cutoff has proven to be highly challenging. In a survey on the topic, Diaconis [12] wrote ‘proof of a cutoff is a difficult, delicate affair, requiring detailed knowledge of the chain, such as all eigenvalues and eigenvectors’. It is therefore worth noting the significant gap between the strength of the results regarding cutoff achieved using information percolation, and those that existed previously.

Previous to [11], the best result known for general graphs was that cutoff occurs with a $\mathcal{O}(1)$ window in the simple case when $\beta = 0$ [13]. However, no results were known for $\beta > 0$, despite a conjecture by Levin et al. in 2009 [8, Section 23.2] that cutoff occurs on any sequence of transitive graphs when the mixing time is of order $\log n$ (as one would expect when $\beta < c_0$ for some $c_0 > 0$ that depends on the sequence of graphs). On lattices, the first results to appear were due to Lubetzky and Sly in 2013 who established cutoff up to the critical temperature for dimensions $d \leq 2$ with only a $\mathcal{O}(\log \log n)$ window [14].

Using information percolation, Lubetzky and Sly proved the existence of cutoff for the continuous time Glauber dynamics for the Ising model with an $\mathcal{O}(1)$ window on \mathbb{Z}^d for all temperatures up to the critical temperature. In a companion paper [15], they extended this result to include any graph for sufficiently high temperature. Since these papers, information percolation has also been used to establish cutoff for the Swendsen-Wang dynamics on the lattice [16], suggesting that the technique is effective on a broader class of problems than simply Glauber dynamics for Ising.

2.3.2 The framework

At its core, information percolation is a way of tracking how the dependencies of the final spins of the Glauber heat-bath dynamics percolate through the graph over time. These dependencies are traced backwards through time from some designated time t^* on the space-time slab $V \times [0, t^*]$ (see Figure 2.1 for example) to create the update history. These histories are made in such a way so that, if for any $j \in V$ no path exists connecting (i, t^*) to $(j, 0)$, then the spin of i does not depend on the initial state (and thus at time t^* vertex i takes $+1$ and -1 spins with equal probability by symmetry). The main constructs used to create this history are the update sequence, and the update support function which we will now define.



Figure 2.1 – A section of the space-time slab $V \times [0, t^*]$ along with a typical appearance of the update histories for two vertices on the cycle. Time runs vertically from bottom to top, and the vertices are represented by circles, laid out horizontally. If there is a path in the update history of v between points (u, t) and (v, t^*) , then the spin of v at time t^* depends on the spin of u at time t . In this example, since there is no path from vertex (i, t^*) to time 0, the final spin at i does not depend on the initial configuration whereas the final spin at j does.

2.3.2.1 The update sequence

Recalling our random mapping representation from Section 2.2.2, we can encode an update of our coupled process with the tuple (\mathcal{V}, U, t) , where t is the time of the update, \mathcal{V} is the vertex that is updated, and U is the value of the uniform random variable that tells us whether \mathcal{V} is a plus or minus according to (2.9). The *update sequence* along an interval $(t_0, t_1]$ is the set of these tuples with $t_0 < t \leq t_1$. Given the state of our Markov Chain at time t_0 , Y_{t_0} , the update sequence along $(t_0, t_1]$ contains all the information we need to construct Y_{t_1} . In particular, given the update sequence along the interval $(0, t_1]$, Y_{t_1} is a deterministic function of Y_0 .

2.3.2.2 The update support function

Given the update sequence along the interval $(t_1, t_2]$, the *update support function*, $\mathcal{F}(A, t_1, t_2)$, is the minimal set of vertices whose spins at time t_1 determine the spins of the vertices in A at time t_2 . That is, $i \in \mathcal{F}(A, t_1, t_2)$ if and only if there exist states $Y_{t_1}, Y'_{t_1} \in \{-1, +1\}^V$

that differ only at i and such that when we construct Y_{t_2} and Y'_{t_2} using the update sequence, $Y_{t_2} \neq Y'_{t_2}$.

In particular, if $\mathcal{F}(i, 0, t) = \emptyset$ then the spin at vertex i at time t does not depend on the initial state and so for any two coupled chains Y and Y' , $Y_t[i] = Y'_t[i]$. As a consequence of the monotonicity of our coupling, we can make the stronger statement that $\mathcal{T}_t[i] = \mathcal{B}_t[i]$ if and only if $\mathcal{F}(i, 0, t) = \emptyset$ which of course means that

$$\mathbb{P}[\mathcal{T}_t[i] \neq \mathcal{B}_t[i]] = \mathbb{P}[\mathcal{F}(i, 0, t) \neq \emptyset]. \quad (2.57)$$

For ease of notation, we will often use the shorthand

$$\mathcal{H}_i(t) := \mathcal{F}(i, t, t^*). \quad (2.58)$$

where t^* is some target time that should be clear from context. We call this the *update history of vertex i at time t* . Tracing $\mathcal{H}_i(t)$ backwards in time from t^* produces a subgraph of $\Omega \times [0, t^*]$ which we write as \mathcal{H}_i and which we simply call the *update history of vertex i* . To be slightly more precise, to produce \mathcal{H}_i we connect (j, t) to (j, t') if $j \in \mathcal{H}_i(t)$ and there are no updates of j along $(t', t]$ and we connect (j, t) to (j', t) if there was an update at (j, t) , $j \in \mathcal{H}_i(t)$, $j' \notin \mathcal{H}_i(t)$, and $j' \in \mathcal{H}_i(t + \epsilon)$ for any sufficiently small $\epsilon > 0$.

To give some intuition to the definitions above, consider how we might construct the update history of a vertex i from some target time t^* . We have at our disposal the update sequence along $(0, t^*]$ which we place in order of decreasing time. If vertex i does not appear in the update sequence then we create a temporal edge between (i, t^*) and $(i, 0)$ and our update history is complete - vertex i was never updated and so it simply takes its initial value. Otherwise, we create temporal edge between (i, t^*) and (i, t_i) where t_i is the last time vertex i was updated. At this point we note from (2.9) that the spin that vertex i takes due to this update depends on the spins of its neighbours. So we add spatial edges from (i, t_i) to (j, t_i) for each $j \sim i$. Finally, we can iterate this process for each neighbour until every history has reached time 0.

In Figure 2.2 we have followed this procedure to show how we might create the update history from a single vertex on the cycle. This construction certainly contains every vertex that might influence the final spin at i , that is, it contains \mathcal{H}_i as a subgraph. However, it is possible for updates to occur that do not depend on neighbouring spins. These updates cause temporal edges leading up to them to terminate without branching out to the neighbouring vertices. These type of updates are called *oblivious updates*.



Figure 2.2 – A naive construction of the update history of i . Each update (\mathcal{V}, U, t) in the update sequence is represented by a $*$ at (\mathcal{V}, t) .

2.3.2.3 Oblivious updates

Generally speaking, an update to a vertex is oblivious if we do not need to know the configuration of its neighbours to determine the spin of that vertex. More precisely, an update, (\mathcal{V}, U, t) , is oblivious if

$$f(\sigma, \mathcal{V}, U)[\mathcal{V}] = f(\sigma', \mathcal{V}, U)[\mathcal{V}] \quad (2.59)$$

for all $\sigma, \sigma' \in \Omega$, where f is as defined in (2.9).

Consider how these updates occur under our random mapping representation. Let Δ_i denote the degree of a vertex i . Recalling (2.7),

$$\frac{e^{-\beta\Delta_i}}{e^{\beta\Delta_i} + e^{-\beta\Delta_i}} \leq p_i(\sigma) \leq \frac{e^{\beta\Delta_i}}{e^{\beta\Delta_i} + e^{-\beta\Delta_i}}, \quad (2.60)$$

with equality holding for the lower and upper limits when the neighbours have spins all minus and all plus respectively. So for a particular update (\mathcal{V}, U, t) , if $U \leq \frac{e^{-\beta\Delta_{\mathcal{V}}}}{e^{\beta\Delta_{\mathcal{V}}} + e^{-\beta\Delta_{\mathcal{V}}}}$ then \mathcal{V} is updated to a plus regardless of the configuration of its neighbours. Hence (\mathcal{V}, U, t) is an oblivious update. Similarly, if $U > \frac{e^{\beta\Delta_{\mathcal{V}}}}{e^{\beta\Delta_{\mathcal{V}}} + e^{-\beta\Delta_{\mathcal{V}}}}$ then \mathcal{V} is updated to a minus regardless of the configuration of its neighbours and hence (\mathcal{V}, U, t) is an oblivious update. It is easy to see that these are the only types of oblivious updates.

The rate of these updates at vertex i is

$$\theta_i = 1 - \left(\frac{e^{\beta\Delta_i}}{e^{\beta\Delta_i} + e^{-\beta\Delta_i}} - \frac{e^{-\beta\Delta_i}}{e^{\beta\Delta_i} + e^{-\beta\Delta_i}} \right) \quad (2.61)$$

$$= 1 - \tanh(\beta\Delta_i). \quad (2.62)$$

If G is a Δ -regular graph (as will be the case in the following chapters) then we can drop the subscript and write $\theta = 1 - \tanh(\beta\Delta)$ for the rate of oblivious updates at each vertex.

As noted earlier, oblivious updates cause temporal edges leading up to them in the update history to terminate. If $j \in \mathcal{H}_i(t)$, then an oblivious update (j, u, t) removes j from $\mathcal{H}_i(t)$ without adding any of its neighbours. In Figure 2.3 we construct an update history from a single vertex i as in Figure 2.2, but this time terminate branches at oblivious updates. To help us represent the updates in our update sequence more precisely, note that on the cycle, the function defined in (2.9) can be rewritten as

$$\sigma'[i] = \begin{cases} 1 & U \leq \theta/2, \\ \sigma[i-1] \vee \sigma[i+1] & \theta/2 < U \leq 1/2, \\ \sigma[i-1] \wedge \sigma[i+1] & 1/2 < U \leq 1 - \theta/2, \\ -1 & U > \theta/2. \end{cases} \quad (2.63)$$

We can therefore represent each update (\mathcal{V}, U, t) in the update sequence by placing at (\mathcal{V}, t) one of the symbols $+$, \vee , \wedge , or $-$ chosen according to U . We then trace back from time t^* , branching to either side when we encounter a \vee or \wedge , and terminating whenever we encounter a $+$ or $-$.

It is worth remarking that oblivious updates are not necessarily the only updates that can shrink the size of the update history of i (see for example Figure 2.4). However, for our analysis they will be the only such updates we will be concerned with. Indeed, in Chapter 3 we will use a different coupling so that these are the only updates that shrink the size of the update history, and in Chapter 4 we will use an alternative construction that bounds the true update history, in which updates are either oblivious or branch out to all Δ neighbours.



Figure 2.3 – The update sequence for a section of the cycle and the corresponding update history from vertex i . For this particular update sequence, i takes a final spin of $+1$ regardless of the initial configuration.



Figure 2.4 – A non-oblivious update that shrinks the size of the update history. On the right is written the final spin of x_3 as a function of the configuration at that time. The update $x_3 \mapsto x_2 \vee x_4$ causes the entire function to collapse to x_4 , and so removes x_1 and x_3 from the update history.

Chapter 3

The Coupling Time on the Cycle

In this chapter we consider the Ising heat-bath Glauber dynamics (as described in Section 2.2.1) on the cycle $G_n = (\mathbb{Z}/n\mathbb{Z})$. The object of interest is the coupling time, T_n , which was defined in Section 2.2.2 but whose definition will be modified slightly in Section 3.1 to allow for simpler analysis. The main result establishes that T_n converges in distribution to a Gumbel distribution at all temperatures. This confirms, for $d = 1$, a conjecture by Collecchio et al. that the coupling time of the Ising heat-bath process on the lattice $G_L = (\mathbb{Z}/L\mathbb{Z})^d$ converges to a Gumbel distribution as $L \rightarrow \infty$ for all $\beta < \beta_C$ [17, Conjecture 7.1] (We treat higher dimensions, and more generally any vertex transitive graphs, in Chapter 4).

Theorem 3.1. *Let T_n be the coupling time for the continuous-time Ising heat-bath Glauber dynamics for the zero-field ferromagnetic Ising model on the cycle $(\mathbb{Z}/n\mathbb{Z})$. Then for any inverse-temperature β ,*

$$\lim_{n \rightarrow \infty} \mathbb{P} \left[T_n < \frac{z + \ln n}{\theta} \right] = e^{-\lambda e^{-z}} \quad (3.1)$$

where $\theta = 1 - \tanh(2\beta)$ and λ is a positive constant bounded by

$$\sqrt{\frac{\theta}{4 - 3\theta}} \leq \lambda \leq 1. \quad (3.2)$$

We postpone the proof of Theorem 3.1 until Section 3.3.

3.1 Information percolation on the cycle

On the cycle, we will use a different coupling of \mathcal{T}_t and \mathcal{B}_t via a new set of update rules that will replace those from (2.9). The new update rules simplify our update histories

greatly by ensuring that each of the update histories never contain more than one vertex at any one time. However, we must be cautious. The coupling time is not just a property of the heat-bath dynamics, but also of the specific coupling we chose. Hence, we will have to verify that switching to our new rules does not change the distribution of T_n .

[UP TO HERE]

The new update rules state that when vertex i updates, a spin σ'_i is chosen via

$$\sigma'_i = \begin{cases} +1 & U < \theta/2, \\ \sigma_{i-1} & \theta/2 \leq U < 1/2, \\ \sigma_{i+1} & 1/2 \leq U < 1 - \theta/2, \\ -1 & U \geq 1 - \theta/2. \end{cases} \quad (3.3)$$

where $U \in [0, 1]$ is an independent uniform random variable as before. It is easy to see that these update rules give rise to the same transition rates as those in (2.9). To show that the coupling time is unchanged, it is sufficient to verify that the joint jump probabilities of $(\mathcal{T}[i], \mathcal{B}_t[i])$ are unchanged for each possible configuration of spins of vertices $i - 1$ and $i + 1$. There are only nine possible configurations for the two neighbours of i in the top and bottom chain since $\mathcal{B}_t[i] \leq \mathcal{T}[i], \forall t$. Likewise, there are only three possible configurations for the updated spins $(\mathcal{T}[i]', \mathcal{B}_t[i']')$. Hence, given vertex i updates at time t , we can easily calculate all the required jump probabilities as shown in Table 3.1. These are unchanged whether using (2.9) or (3.3) and so the new rules do not change the coupled dynamics.

3.1.1 Update histories on the cycle

Under the update rules in (3.3), each time a vertex is updated, it is either an oblivious update with probability θ , or it takes the spin of a uniformly chosen neighbour. So as t decreases from t^* , $\mathcal{H}_i(t)$ is a continuous-time random walk that dies at rate θ , moves left at rate $(1 - \theta)/2$, and moves right at rate $(1 - \theta)/2$. The probability that $\mathcal{H}_i(0) \neq \emptyset$ is simply the probability that the continuous-time random walk survives until time $t = 0$. So recalling (2.57)

$$\mathbb{P}[\mathcal{B}_{t^*}[i] \neq \mathcal{T}_{t^*}[i]] = \mathbb{P}[\mathcal{H}_i(0) \neq \emptyset] = e^{-\theta t^*}. \quad (3.4)$$

$\mathbb{P}[(\mathcal{T}_t[i]', \mathcal{B}_t[i']) = \cdot]$		(1,1)	(1,-1)	(-1,-1)
$\mathcal{T}_t = \cdot$	$\mathcal{B}_t = \cdot$			
$(\dots, 1, \sigma_i, 1, \dots)$	$(\dots, 1, \sigma_i, 1, \dots)$	$1 - \theta$	0	$\frac{\theta}{2}$
$(\dots, 1, \sigma_i, 1, \dots)$	$(\dots, 1, \sigma_i, -1, \dots)$	$\frac{1}{2}$	$\frac{1-\theta}{2}$	$\frac{\theta}{2}$
$(\dots, 1, \sigma_i, 1, \dots)$	$(\dots, -1, \sigma_i, 1, \dots)$	$\frac{1}{2}$	$\frac{1-\theta}{2}$	$\frac{\theta}{2}$
$(\dots, 1, \sigma_i, 1, \dots)$	$(\dots, -1, \sigma_i, -1, \dots)$	$\frac{\theta}{2}$	$1 - \theta$	$\frac{\theta}{2}$
$(\dots, 1, \sigma_i, -1, \dots)$	$(\dots, 1, \sigma_i, -1, \dots)$	$\frac{1}{2}$	0	$\frac{1}{2}$
$(\dots, 1, \sigma_i, -1, \dots)$	$(\dots, -1, \sigma_i, -1, \dots)$	$\frac{\theta}{2}$	$\frac{1-\theta}{2}$	$\frac{1}{2}$
$(\dots, -1, \sigma_i, 1, \dots)$	$(\dots, -1, \sigma_i, 1, \dots)$	$\frac{1}{2}$	0	$\frac{1}{2}$
$(\dots, -1, \sigma_i, 1, \dots)$	$(\dots, -1, \sigma_i, -1, \dots)$	$\frac{\theta}{2}$	$\frac{1-\theta}{2}$	$\frac{1}{2}$
$(\dots, -1, \sigma_i, -1, \dots)$	$(\dots, -1, \sigma_i, -1, \dots)$	$\frac{\theta}{2}$	0	$1 - \theta$

Table 3.1 – Probabilities of updating from $(\mathcal{T}_t, \mathcal{B}_t)$ to $(\mathcal{T}_t', \mathcal{B}_t')$ given vertex i updates at time t .

3.2 Compound Poisson Approximation

Fix z and a time of interest, $t_* = (z + \ln n)/\theta$. For each vertex $i \in G$, we define indicators

$$X_i = \begin{cases} 1 & \mathcal{B}_{t_*}[i] \neq \mathcal{T}_{t_*}[i], \\ 0 & \mathcal{B}_{t_*}[i] = \mathcal{T}_{t_*}[i] \end{cases} \quad (3.5)$$

and set $W = \sum_{i \in V} X_i$. Note that from (3.4) we get

$$\mathbb{P}[X_i = 1] = e^{-\theta t_*} = \frac{e^{-z}}{n}. \quad (3.6)$$

The random variable W is closely related to the distribution of the coupling time T in that the events $\{W = 0\}$ and $\{T \leq t_*\}$ are the same. We will show that the limiting distribution of W as n increases is compound Poisson using Theorem 3.2 which we have taken from [18] which in turn is based on Stein's method for the compound Poisson distribution, introduced in [19]. Before stating the theorem as it applies to our problem, there are a few more quantities we need to define.

For each $i \in V$, decompose W into $W = X_i + U_i + Z_i + W_i$ where

$$U_i = \sum_{j \in B_i} X_j, \quad Z_i = \sum_{j \in C_i} X_j, \quad W_i = \sum_{j \in D_i} X_j. \quad (3.7)$$

and B_i, C_i , and D_i are the vertex sets

$$B_i = \{j \neq i : |j - i| \leq b_n\}, \quad (3.8)$$

$$C_i = \{j \notin B_i \cup \{i\} : |j - i| \leq c_n\}, \quad (3.9)$$

$$D_i = V \setminus (B_i \cup C_i \cup \{i\}). \quad (3.10)$$

We have some freedom in choosing b_n and c_n , but they must be chosen such that various quantities go to zero as $n \rightarrow \infty$. One choice that will work in our circumstances is $b_n = \ln(n)$ and $c_n = \ln(n)^2$.

Define the following which are the parameters of the approximating compound Poisson distribution to W .

$$\lambda = \sum_{i \in V} \mathbb{E} \left[\frac{X_i}{X_i + U_i} I[X_i + U_i \geq 1] \right], \quad (3.11)$$

$$\mu_l = \frac{1}{l\lambda} \sum_{i \in V} \mathbb{E} [X_i I[X_i + U_i = l]], \quad l \geq 1. \quad (3.12)$$

Also define quantities

$$\delta_1 = \sum_{i \in V} \sum_{k \geq 0} \mathbb{P}[X_i = 1, U_i = k] \mathbb{E} \left| \frac{\mathbb{P}[X_i = 1, U_i = k | W_i]}{\mathbb{P}[X_i = 1, U_i = k]} - 1 \right|, \quad (3.13)$$

$$\delta_4 = \sum_{i \in V} (\mathbb{E}[X_i Z_i] + \mathbb{E}[X_i] \mathbb{E}[X_i + U_i + Z_i]). \quad (3.14)$$

which we require to vanish as $n \rightarrow \infty$.

The following theorem (reworked from [18]) bounds the distance between the distributions of W and the approximating compound Poisson.

Theorem 3.2 ([18]). *Let W , λ , μ , δ_1 and δ_4 be as defined above. Then there exist constants $C_1 = C_1(\lambda, \mu)$ and $C_2 = C_2(\lambda, \mu)$ such that*

$$d_{\text{TV}}(\mathcal{L}(W), \text{CP}(\lambda, \mu)) \leq C_1 \delta_1 + C_2 \delta_4. \quad (3.15)$$

As an immediate corollary, and from the equivalence of the events $\{W = 0\}$ and $\{T \leq t^*\}$, we get that

$$\left| \mathbb{P} \left[T \leq \frac{z + \ln(n)}{\theta} \right] - e^{-\lambda} \right| \leq C_1 \delta_1 + C_2 \delta_4. \quad (3.16)$$

3.3 Proof of Theorem 3.1

The proof of Theorem 3.1 comes as a result of equation (3.16) along with Lemmas 3.3, 3.4, and 3.5 which bound the various quantities required.

Lemma 3.3. *Using the above setup*

$$\sqrt{\frac{\theta}{4-3\theta}}e^{-z} \leq \lim_{n \rightarrow \infty} \lambda \leq e^{-z}. \quad (3.17)$$

Proof.

$$\lambda = \sum_{i \in V} \mathbb{E} \left[\frac{X_i}{X_i + U_i} I[X_i + U_i \geq 1] \right] \quad (3.18)$$

$$= \sum_{i=1}^n \mathbb{P}(X_i = 1) \mathbb{E} \left[\frac{1}{1 + U_i} | X_i = 1 \right] \quad (3.19)$$

$$= \sum_{i=1}^n \frac{e^{-z}}{n} \mathbb{E} \left[\frac{1}{1 + U_i} | X_i = 1 \right] \quad (3.20)$$

$$= e^{-z} \mathbb{E} \left[\frac{1}{1 + U_i} | X_i = 1 \right] \quad (3.21)$$

where we have used that X_i is zero-one, (3.6), and the transitivity of the graph. Clearly

$$\mathbb{E} \left[\frac{1}{1 + U_i} | X_i = 1 \right] \leq 1 \quad (3.22)$$

and so $\lambda \leq e^{-z}$.

By Jensen's inequality

$$\mathbb{E} \left[\frac{1}{1 + U_i} | X_i = 1 \right] \geq \frac{1}{\mathbb{E}[1 + U_i | X_i = 1]} \quad (3.23)$$

$$= \frac{1}{1 + \mathbb{E}[U_i | X_i = 1]}. \quad (3.24)$$

so in order to find a lower bound for λ we will find an upper bound to $\mathbb{E}[U_i | X_i = 1]$. Now

$$\mathbb{E}[U_i | X_i = 1] = \sum_{j \in B_i} \mathbb{P}[X_j = 1 | X_i = 1] \quad (3.25)$$

$$= \sum_{k=1}^{b_n} \sum_{|j-i|=k} \mathbb{P}[X_j = 1 | X_i = 1] \quad (3.26)$$

$$= 2 \sum_{k=1}^{b_n} \mathbb{P}[X_{i+k} = 1 | X_i = 1] \quad (3.27)$$

where we have used the symmetry of X_{i+k} and X_{i-k} in the last step. From Lemma 3.8,

$$\mathbb{E}[U_i | X_i = 1] \leq 2 \sum_{k=1}^{b_n} \left(\frac{e^{-z}}{n} + \left(\frac{2 - \theta - \sqrt{4\theta - 3\theta^2}}{2(1 - \theta)} \right)^k \right) \quad (3.28)$$

$$< 2 \sum_{k=1}^{b_n} \frac{e^{-z}}{n} + 2 \sum_{k=1}^{\infty} \left(\frac{2 - \theta - \sqrt{4\theta - 3\theta^2}}{2(1 - \theta)} \right)^k \quad (3.29)$$

$$= \frac{2b_n}{n} e^{-z} + \sqrt{\frac{4}{\theta} - 3} - 1. \quad (3.30)$$

Finally, as $n \rightarrow \infty$ the first term vanishes and

$$\lim_{n \rightarrow \infty} \lambda \geq \sqrt{\frac{\theta}{4 - 3\theta}} e^{-z}. \quad (3.31)$$

□

Lemma 3.4.

$$\lim_{n \rightarrow \infty} \delta_1 = 0 \quad (3.32)$$

Proof.

$$\delta_1 = \sum_{i=1}^n \sum_{k=0}^{2b_n} \mathbb{P}[X_i = 1, U_i = k] \mathbb{E} \left| \frac{\mathbb{P}[X_i = 1, U_i = k | W_i]}{\mathbb{P}[X_i = 1, U_i = k]} - 1 \right| \quad (3.33)$$

$$= n \sum_{k=0}^{2b_n} \mathbb{E} |\mathbb{P}[X_i = 1, U_i = k | W_i] - \mathbb{P}[X_i = 1, U_i = k]| \quad (3.34)$$

Let A be the event that the history of a vertex in D_i merges with the history of a vertex in $B_i \cup \{i\}$. More formally,

$$A = \{\exists j \in B_i \cup \{i\}, l \in D_i : \mathcal{H}_j \cap \mathcal{H}_l \neq \emptyset\}. \quad (3.35)$$

We note that if A does not happen, then W_i cannot affect X_i or U_i . That is,

$$\mathbb{P}[X_i = 1, U_i = j | A^c, W_i] = \mathbb{P}[X_i = 1, U_i = j | A^c]. \quad (3.36)$$

Continuing on from (3.34), we split the probabilities into

$$\delta_1 = n \sum_{k=0}^{2b_n} \mathbb{E} \left| \mathbb{P}[X_i = 1, U_i = k | W_i, A] \mathbb{P}[A | W_i] - \mathbb{P}[X_i = 1, U_i = k | A] \mathbb{P}[A] + \right. \quad (3.37)$$

$$\left. \mathbb{P}(X_i = 1, U_i = k | A^c) (\mathbb{P}[A^c | W_i] - \mathbb{P}[A^c]) \right| \leq n(2b_n + 1) \mathbb{E} \left[\mathbb{P}[A | W_i] + \mathbb{P}[A] + \left| \mathbb{P}[A^c | W_i] - \mathbb{P}[A^c] \right| \right] \quad (3.38)$$

$$= n(2b_n + 1) \mathbb{E} [\mathbb{P}[A | W_i] + \mathbb{P}[A] + |1 - \mathbb{P}[A | W_i] - (1 - \mathbb{P}[A])|] \quad (3.39)$$

$$\leq n(2b_n + 1) \mathbb{E} [\mathbb{P}[A | W_i] + \mathbb{P}[A] + \mathbb{P}[A | W_i] + \mathbb{P}[A]] \quad (3.40)$$

$$= 2n(2b_n + 1) (\mathbb{E}[\mathbb{P}[A | W_i]] + \mathbb{P}[A]) \quad (3.41)$$

$$= 4n(2b_n + 1) \mathbb{P}[A] \quad (3.42)$$

Let $A_{j,k}$ denote the event that the histories of vertices j and k merge. That is,

$$A_{j,k} = \{\mathcal{H}_j \cap \mathcal{H}_k \neq \emptyset\}. \quad (3.43)$$

By a union bound,

$$\delta_1 \leq 4n(2b_n + 1) \sum_{j \in B_i \cup \{i\}} \sum_{k \in D_i} \mathbb{P}[A_{j,k}] \quad (3.44)$$

$$\leq 8n^2(2b_n + 1)^2 \left(\frac{1 - \sqrt{\theta(2 - \theta)}}{1 - \theta} \right)^{c_n - b_n} \quad (3.45)$$

by Lemma 3.6. This goes to 0 as $n \rightarrow \infty$. \square

Lemma 3.5.

$$\lim_{n \rightarrow \infty} \delta_4 = 0 \quad (3.46)$$

Proof.

$$\delta_4 = \sum_{i=1}^n (\mathbb{E}[X_i Z_i] + \mathbb{E}[X_i] \mathbb{E}[X_i + U_i + Z_i]) \quad (3.47)$$

$$= \sum_{i=1}^n \mathbb{E}[X_i Z_i] + e^{-z} \sum_{j \in \{i\} \cup B_i \cup C_i} \mathbb{E}[X_j] \quad (3.48)$$

$$= n \mathbb{E}[X_i Z_i] + \frac{2e^{-2z} c_n}{n} \quad (3.49)$$

$$= n \mathbb{P}[X_i = 1] \mathbb{E}[Z_i | X_i = 1] + \frac{2e^{-2z} c_n}{n} \quad (3.50)$$

$$= e^{-z} \mathbb{E}[Z_i | X_i = 1] + \frac{2e^{-2z} c_n}{n} \quad (3.51)$$

Now

$$\mathbb{E}[Z_i | X_i = 1] = \sum_{j \in C_i} \mathbb{P}[X_j = 1 | X_i = 1] \quad (3.52)$$

$$= 2 \sum_{k=b_n+1}^{c_n} \mathbb{P}[X_{i+k} = 1 | X_i = 1] \quad (3.53)$$

From Lemma 3.8,

$$\mathbb{E}[Z_i | X_i = 1] \leq 2 \sum_{k=b_n+1}^{c_n} \left(\frac{e^{-z}}{n} + 2 \left(\frac{2 - \theta - \sqrt{4\theta - 3\theta^2}}{2(1 - \theta)} \right)^k \right) \quad (3.54)$$

$$\leq \frac{2(c_n - b_n)e^{-z}}{n} + 4(c_n - b_n) \left(\frac{2 - \theta - \sqrt{4\theta - 3\theta^2}}{2(1 - \theta)} \right)^{b_n+1}. \quad (3.55)$$

Altogether

$$\delta_4 \leq \frac{2(c_n - b_n)e^{-z}}{n} + 4(c_n - b_n) \left(\frac{2 - \theta - \sqrt{4\theta - 3\theta^2}}{2(1 - \theta)} \right)^{b_n+1} + \frac{2e^{-2z}c_n}{n} \quad (3.56)$$

which goes to 0 as $n \rightarrow \infty$. \square

3.3.1 Additional Lemmas

Lemma 3.6. *Let $A_{i,j}$ be the event that the update history of vertex i merges with the update history of vertex j . Then*

$$\mathbb{P}[A_{i,j}] \leq 2 \left(\frac{1 - \sqrt{\theta(2 - \theta)}}{1 - \theta} \right)^k \quad (3.57)$$

where $k = |i - j|$.

Proof. We note that, while the update histories survive, the distance between the update histories of i and j is a birth and death process that starts at $k = |i - j|$ and has birth and death rates, $\lambda = \mu = 1 - \theta$. Let $P(t)$ be such a process and define $s_0 = \inf\{t : P(t) = 0\}$ to be the first time the process reaches zero (this corresponds to the update histories merging). Let s_d be exponentially distributed with rate 2θ (this corresponds to the first time that one of the update histories dies). Then

$$\mathbb{P}[A_{i,j}] \leq 2\mathbb{P}_k(s_0 < s_d) \quad (3.58)$$

where \mathbb{P}_k indicates that $P(0) = k$. The factor of two comes from the fact that the update histories may meet by going the other direction around the cycle.

At any time before s_d there are three possibilities for what can happen to P next. Either the next event is a birth with probability $(1 - \theta)/2$, the next event is a death with the same probability or we reach time s_d with probability θ . Writing $\zeta_k = \mathbb{P}_k(s_0 < s_d)$ this gives us the recurrence relation

$$\zeta_k = \frac{1 - \theta}{2} \zeta_{k-1} + \frac{1 - \theta}{2} \zeta_{k+1} \quad (3.59)$$

which is subject to the conditions

$$\zeta_0 = 1 \quad (3.60)$$

$$\zeta_k \leq 1, \forall k \in \mathbb{N}. \quad (3.61)$$

This recurrence has characteristic equation

$$x^2 - \frac{2}{1 - \theta}x + 1 = 0 \quad (3.62)$$

which has roots

$$r_1 = \frac{1 + \sqrt{\theta(2 - \theta)}}{1 - \theta} \quad (3.63)$$

$$r_2 = \frac{1 - \sqrt{\theta(2 - \theta)}}{1 - \theta} \quad (3.64)$$

and so

$$\zeta_k = ar_1^k + br_2^k \quad (3.65)$$

where a and b are constants to be determined from (3.60) and (3.61). We note that $r_1 \geq 1, \forall \theta \in [0, 1]$ and so from (3.61) we have that $a = 0$. Finally from (3.60), $b = 1$ and so

$$\zeta_k = \left(\frac{1 - \sqrt{\theta(2 - \theta)}}{1 - \theta} \right)^k. \quad (3.66)$$

□

Lemma 3.7. *Let $A_{i,j}$ be the event that the update history of vertex i merges with the update history of vertex j . Then*

$$\mathbb{P}[A_{i,j} | X_j = 1] \leq 2 \left(\frac{2 - \theta - \sqrt{4\theta - 3\theta^2}}{2(1 - \theta)} \right)^k \quad (3.67)$$

where $k = |i - j|$.

Proof. We note that, while the update histories survive, the distance between the update histories of i and j is a birth and death process that starts at $k = |i - j|$ and has birth and death rates, $\lambda = \mu = 1 - \theta$. Let $P(t)$ be such a process and define $s_0 = \inf\{t : P(t) = 0\}$ to be the first time the process reaches zero (this corresponds to the update histories merging). Let s_d be exponentially distributed with rate θ (this corresponds to the update history of vertex i dying). Then

$$\mathbb{P}[A_{i,j}|X_j = 1] \leq 2\mathbb{P}_k(s_0 < s_d) \quad (3.68)$$

where \mathbb{P}_k indicates that $P(0) = k$. The factor of two comes from the fact that the update histories may meet by going the other direction around the cycle.

At any time before s_d there are three possibilities for what can happen to P next. Either the next event is a birth with probability $(1 - \theta)/(2 - \theta)$, the next event is a death with the same probability or we reach time s_d with probability $\theta/(2 - \theta)$. Writing $\zeta_k = \mathbb{P}_k(s_0 < s_d)$ this gives us the recurrence relation

$$\zeta_k = \frac{1 - \theta}{2 - \theta}\zeta_{k-1} + \frac{1 - \theta}{2 - \theta}\zeta_{k+1} \quad (3.69)$$

which is subject to the conditions

$$\zeta_0 = 1 \quad (3.70)$$

$$\zeta_k \leq 1, \forall k \in \mathbb{N}. \quad (3.71)$$

This recurrence has characteristic equation

$$x^2 - \frac{2 - \theta}{1 - \theta}x + 1 = 0 \quad (3.72)$$

which has roots

$$r_1 = \frac{2 - \theta + \sqrt{4\theta - 3\theta^2}}{2(1 - \theta)} \quad (3.73)$$

$$r_2 = \frac{2 - \theta - \sqrt{4\theta - 3\theta^2}}{2(1 - \theta)} \quad (3.74)$$

and so

$$\zeta_k = ar_1^k + br_2^k \quad (3.75)$$

where a and b are constants to be determined from (3.70) and (3.71). We note that $r_1 \geq 1, \forall \theta \in [0, 1]$ and so from (3.71) we have that $a = 0$. Finally from (3.70), $b = 1$ and so

$$\zeta_k = \left(\frac{2 - \theta - \sqrt{4\theta - 3\theta^2}}{2(1 - \theta)} \right)^k. \quad (3.76)$$

□

Lemma 3.8.

$$\mathbb{P}[X_{i+k} = 1 | X_i = 1] \leq \frac{e^{-z}}{n} + 2 \left(\frac{2 - \theta - \sqrt{4\theta - 3\theta^2}}{2(1 - \theta)} \right)^k. \quad (3.77)$$

Proof. There are two ways in which the update history of vertex $i + k$ can survive until time 0. The update history can survive without intersecting with the update history of vertex i or the update history of vertex $i + k$ can survive long enough to merge with the update history of vertex i (whose survival we are conditioning on). (Note that these events are not mutually exclusive as the update history of vertex $i + k$ could merge with the update history of vertex i after it reaches time 0.) So we have

$$\mathbb{P}[X_{i+k} = 1 | X_i = 1] \leq \mathbb{P}[X_{i+k} = 1] + \mathbb{P}[A_{i,i+k} | X_i = 1]. \quad (3.78)$$

The result follows from (3.6) and Lemma 3.7. □

Chapter 4

The Coupling Time on Vertex Transitive Graphs

In this chapter we prove the following theorem.

Conjecture 4.1. *Let T_L be the coupling time for the continuous-time Ising heat-bath dynamics for the zero-field ferromagnetic Ising model on the torus $(\mathbb{Z}/L\mathbb{Z})^d$. Then for any small enough inverse-temperature β ,*

$$\lim_{L \rightarrow \infty} \mathbb{P}[T_L < a_L z + b_L] = e^{-e^{-z}} \quad (4.1)$$

where a_L and b_L have yet to be determined.

Proof.

□

4.1 Information Percolation in higher dimensions

In the previous chapter, we showed that on the cycle, there was a coupling that made the update history of a single vertex to be a continuous-time random walk that died at rate θ . On lattices of dimension $d > 2$, we can no longer use this coupling and so the updates histories are significantly more complex.

Recall from Section 2.3.2.2 that given a target time t^* , the update history of a vertex set A at time t , $\mathcal{H}_A(t)$, is the set of vertices whose spins at time t determine the spins of A at time t^* . Developing this history backwards in time from $t = t^*$ produces a subgraph of $\Omega \times [0, t^*]$ which we write as \mathcal{H}_A and call the update history of vertex set A . This history can be constructed using the update sequence along $(t, t^*]$.

In practise, we may choose to construct this history as follows: For each $i \in A$, create a temporal edge between (i, t^*) and (i, t_i) where t_i is the time of the latest update to i (or 0 if i is never updated). Then for each update (i, u, t_i) , we either terminate the edge if u is such that the update is oblivious, or we add spatial branches to each of the neighbours of i . We repeat this process recursively for the neighbours of i until every branch has been terminated due to an oblivious update or has reached time 0.

However, it is possible for vertices to be removed from $\mathcal{H}_A(t)$ from updates that are not oblivious. [PUT EXAMPLE IN]. Since our method above for constructing the history does not take this into account, the history it produces will possibly be larger than \mathcal{H}_A . To ensure a distinction between the two, the history that results from the above construction we will denote $\hat{\mathcal{H}}_A$, and likewise $\hat{\mathcal{H}}_A(t)$ for the history at time t that results from the above construction. We have that

$$\mathcal{H}_A(t) \subseteq \hat{\mathcal{H}}_A(t) \quad (4.2)$$

and also that \mathcal{H}_A is a subgraph of $\hat{\mathcal{H}}_A$.

4.1.1 Magnetization

One quantity which we used multiple times in Chapter 3 was $\mathbb{P}[X_i = 1]$. Although it was not required earlier, we would now like to make clear that this is in fact the magnetization at time t^* .

The magnetization at vertex $i \in V$ at time $t > 0$ is defined to be

$$m_t(i) = \mathbb{E}[\mathcal{T}_t[i]] \quad (4.3)$$

where $(\mathcal{T}_t)_{t \geq 0}$ is the dynamics starting from the all-plus configuration. Given a monotonically coupled chain $(\mathcal{B}_t)_{t \geq 0}$, starting in the all minus configuration and such that $\mathcal{T}_t[i] \geq \mathcal{B}_t[i]$ for all $t \geq 0$ and $i \in V$, we can split up this expectation by conditioning on the event $A_t = \{\mathcal{T}_t[i] \neq \mathcal{B}_t[i]\}$. We obtain that

$$m_t(i) = \mathbb{E}[Y_t^+[i]] \quad (4.4)$$

$$\begin{aligned} &= \mathbb{P}[A_t] \left(\mathbb{P}[Y_t^+[i] = 1 | A_t] - \mathbb{P}[Y_t^+[i] = -1 | A_t] \right) \\ &\quad + \mathbb{P}[A_t^c] \left(\mathbb{P}[Y_t^+[i] = 1 | A_t^c] - \mathbb{P}[Y_t^+[i] = -1 | A_t^c] \right). \end{aligned} \quad (4.5)$$

Now if event A_t^c holds, $\mathcal{T}_t[i] = \mathcal{B}_t[i]$, and so by symmetry vertex i must take values -1 and $+1$ uniformly. Furthermore, by the monotonicity of our coupling, if A_t holds, we

must have that $\mathcal{T}_t[i] = +1$ and $\mathcal{B}_t[i] = -1$. So

$$m_t(i) = \mathbb{P}[A_t]. \quad (4.6)$$

Finally, given a target time t^* , X_i is defined such that $\{X_i = 1\} = A_{t^*}$. So $\mathbb{P}[X_i = 1] = m_{t^*}(i)$. This motivates the following restatement of part of Lemma 2.1 from [11].

Lemma 4.2 ([11], Lemma 2.1). *There exist some constant $c_{\beta,d} > 0$ such that for any $t > 0$,*

$$m_t \leq 2e^{-c_{\beta,d}t} \quad (4.7)$$

Corollary 4.3.

$$\mathbb{P}[X_i = 1] \leq 2e^{-c_{\beta,d}t^*} \quad (4.8)$$

4.2 Setup

Define the time

$$t_c(n) = \inf \left\{ t > 0 : m_t = \frac{1}{n} \right\}. \quad (4.9)$$

Fix z and a time of interest $t^* = t_c(n) + z$.

Lemma 4.4 ([15], Claim 3.3). *On any graph with maximum degree Δ , for any $t, s > 0$ we have*

$$e^{-2s} \leq \frac{\sum_i m_{t+s}[i]^2}{\sum_i m_t[i]^2} \leq e^{-2(1-\beta\Delta)s}. \quad (4.10)$$

The following corollary is then straightforward.

Corollary 4.5. *On any vertex transitive graph with degree Δ , m_{t^*} can be bounded as follows:*

For $z \geq 0$,

$$\frac{e^{-z}}{n} \leq m_{t^*} \leq \frac{e^{-(1-\beta\Delta)z}}{n}. \quad (4.11)$$

For $z \leq 0$,

$$\frac{e^{-(1-\beta\Delta)z}}{n} \leq m_{t^*} \leq \frac{e^{-z}}{n}. \quad (4.12)$$

Corollary 4.6. *On any vertex transitive graph with degree Δ , for $\beta < 1/\Delta$*

$$\ln(n) \leq t_c(n) \leq \frac{\ln(n)}{1 - \beta\Delta} \quad (4.13)$$

4.3 Proof of Theorem 4.1

Lemma 4.7. *Using the above setup*

$$\leq \lim_{n \rightarrow \infty} \lambda \leq nm_{t^*} \quad (4.14)$$

Proof.

$$\lambda = \sum_{i \in V} \mathbb{E} \left[\frac{X_i}{X_i + U_i} I[X_i + U_i \geq 1] \right] \quad (4.15)$$

$$= \sum_{i=1}^n \mathbb{P}(X_i = 1) \mathbb{E} \left[\frac{1}{1 + U_i} | X_i = 1 \right] \quad (4.16)$$

$$= nm_{t^*} \mathbb{E} \left[\frac{1}{1 + U_i} | X_i = 1 \right] \quad (4.17)$$

where we have used that X_i is zero-one, (3.6), and the transitivity of the graph. Clearly

$$\mathbb{E} \left[\frac{1}{1 + U_i} | X_i = 1 \right] \leq 1 \quad (4.18)$$

and so $\lambda \leq nm_{t^*}$.

By Jensen's inequality

$$\mathbb{E} \left[\frac{1}{1 + U_i} | X_i = 1 \right] \geq \frac{1}{\mathbb{E}[1 + U_i | X_i = 1]} \quad (4.19)$$

$$= \frac{1}{1 + \mathbb{E}[U_i | X_i = 1]}. \quad (4.20)$$

so in order to find a lower bound for λ we will find an upper bound to $\mathbb{E}[U_i | X_i = 1]$. Now

$$\mathbb{E}[U_i | X_i = 1] = \sum_{j \in B_i} \mathbb{P}[X_j = 1 | X_i = 1] \quad (4.21)$$

$$= \sum_{k=1}^{b_n} \sum_{|j-i|=k} \mathbb{P}[X_j = 1 | X_i = 1] \quad (4.22)$$

$$\leq \sum_{k=1}^{b_n} \sum_{|j-i|=k} (m_{t^*} + \mathbb{P}[\mathcal{H}_j \cap \mathcal{H}_i \neq \emptyset | X_i = 1]) \quad (4.23)$$

□

Lemma 4.8.

$$\lim_{n \rightarrow \infty} \delta_1 = 0 \quad (4.24)$$

Proof.

$$\delta_1 = \sum_{i=1}^n \sum_{k=0}^{|B_i|} \mathbb{P}[X_i = 1, U_i = k] \mathbb{E} \left| \frac{\mathbb{P}[X_i = 1, U_i = k | W_i]}{\mathbb{P}[X_i = 1, U_i = k]} - 1 \right| \quad (4.25)$$

$$= n \sum_{k=0}^{|B_i|} \mathbb{E} |\mathbb{P}[X_i = 1, U_i = k | W_i] - \mathbb{P}[X_i = 1, U_i = k]| \quad (4.26)$$

Let A be the event that the history of a vertex in D_i merges with the history of a vertex in $B_i \cup \{i\}$. More formally,

$$A = \{\exists j \in B_i \cup \{i\}, l \in D_i : \mathcal{H}_j \cap \mathcal{H}_l \neq \emptyset\}. \quad (4.27)$$

We note that if A does not happen, then W_i cannot affect X_i or U_i . That is,

$$\mathbb{P}[X_i = 1, U_i = j | A^c, W_i] = \mathbb{P}[X_i = 1, U_i = j | A^c]. \quad (4.28)$$

Continuing on from (4.26), we split the probabilities into

$$\delta_1 = n \sum_{k=0}^{|B_i|} \mathbb{E} \left| \mathbb{P}[X_i = 1, U_i = k | W_i, A] \mathbb{P}[A | W_i] - \mathbb{P}[X_i = 1, U_i = k | A] \mathbb{P}[A] + \right. \quad (4.29)$$

$$\left. \mathbb{P}(X_i = 1, U_i = k | A^c) (\mathbb{P}[A^c | W_i] - \mathbb{P}[A^c]) \right|$$

$$\leq n(|B_i| + 1) \mathbb{E} \left[\mathbb{P}[A | W_i] + \mathbb{P}[A] + \left| \mathbb{P}[A^c | W_i] - \mathbb{P}[A^c] \right| \right] \quad (4.30)$$

$$= n(|B_i| + 1) \mathbb{E} [\mathbb{P}[A | W_i] + \mathbb{P}[A] + |1 - \mathbb{P}[A | W_i] - (1 - \mathbb{P}[A])|] \quad (4.31)$$

$$\leq n(|B_i| + 1) \mathbb{E} [\mathbb{P}[A | W_i] + \mathbb{P}[A] + \mathbb{P}[A | W_i] + \mathbb{P}[A]] \quad (4.32)$$

$$= 2n(|B_i| + 1) (\mathbb{E}[\mathbb{P}[A | W_i]] + \mathbb{P}[A]) \quad (4.33)$$

$$= 4n(|B_i| + 1) \mathbb{P}[A] \quad (4.34)$$

By a union bound,

$$\delta_1 \leq 4n(|B_i| + 1) \sum_{j \in B_i \cup \{i\}} \sum_{k \in D_i} \mathbb{P}[\mathcal{H}_j \cap \mathcal{H}_k \neq \emptyset]. \quad (4.35)$$

From Lemma 4.10,

$$\delta_1 \leq 4n^2(|B_i| + 1)^2 \exp(2\alpha) \exp(-\lambda(c_n - b_n)). \quad (4.36)$$

On the torus $(\mathbb{Z}/L\mathbb{Z})^d$, $n = L^d$, $c_n = \log(L)^2$, $b_n = \log(L)$, and $|B_i| \leq C \log(L)^d$. So

$$\delta_1 \leq CL^{2d} \log(L)^{2d} \exp(-\lambda(\log(L)^2 - \log(L))) \quad (4.37)$$

which goes to 0 as $L \rightarrow \infty$. \square

Lemma 4.9.

$$\lim_{n \rightarrow \infty} \delta_4 = 0 \quad (4.38)$$

Proof.

$$\delta_4 = \sum_{i=1}^n (\mathbb{E}[X_i Z_i] + \mathbb{E}[X_i] \mathbb{E}[X_i + U_i + Z_i]) \quad (4.39)$$

$$= n \mathbb{E}[X_i Z_i] + nm_{t^*}^2 (1 + |B_i| + |C_i|) \quad (4.40)$$

$$= nm_{t^*} \mathbb{E}[Z_i | X_i = 1] + nm_{t^*}^2 (1 + |B_i| + |C_i|) \quad (4.41)$$

$$= nm_{t^*} \left(\sum_{j \in C_i} \mathbb{P}[X_j = 1 | X_i = 1] + m_{t^*} (1 + |B_i| + |C_i|) \right) \quad (4.42)$$

$$\leq nm_{t^*} \left(\sum_{j \in C_i} (m_{t^*} + \mathbb{P}[\mathcal{H}_j \cap \mathcal{H}_i \neq \emptyset | X_i = 1] + m_{t^*} (1 + |B_i| + |C_i|)) \right) \quad (4.43)$$

NEED TO PROVE LEMMA 4.11 \square

4.3.1 Additional Lemmas

Lemma 4.10.

$$\mathbb{P}[\mathcal{H}_j \cap \mathcal{H}_k \neq \emptyset] \leq \exp(2\alpha) \exp(-\lambda|j - k|). \quad (4.44)$$

Proof. The following is based on the proof used in Section 3.2 of [20].

We first relax our histories to our alternative construction by observing that

$$\mathbb{P}[\mathcal{H}_j \cap \mathcal{H}_k \neq \emptyset] \leq \mathbb{P}[\hat{\mathcal{H}}_j \cap \hat{\mathcal{H}}_k \neq \emptyset]. \quad (4.45)$$

Let $W_s = |\hat{\mathcal{H}}_{\{j,k\}}(t^* - s)|$ and let $Y_s = \#\left\{((u, t), (v, t)) \in \hat{\mathcal{H}}_{\{j,k\}} : t \in [t^* - s, t^*)\right\}$ count the total number of spatial edges observed in the history by time $t^* - s$. For $\hat{\mathcal{H}}_j$ and $\hat{\mathcal{H}}_k$ to intersect at time $t^* - s$, there must be enough spatial edges for the histories to reach each other. That is, we require that

$$Y_s \geq |i - j|. \quad (4.46)$$

Initially, $W_0 = 2$ and $Y_0 = 0$. Recall that an oblivious update of a vertex causes it to be removed from the history and that a non-oblivious update causes the history to branch out to its Δ neighbours. Oblivious updates occur at rate θW_s and cause W_s to decrease by 1. Non-oblivious updates occur at rate $(1 - \theta)W_s$ and cause both W_s and Y_s to increase by no more than Δ . Therefore we can create a coupled process (\bar{W}_s, \bar{Y}_s) such that $\bar{W}_s \geq W_s$ and $\bar{Y}_s \geq Y_s$ in the following way. We start with $(\bar{W}_s, \bar{Y}_s) = (2, 0)$ and at rate $\theta \bar{W}_s$, \bar{W}_s decreases by 1, and at rate $(1 - \theta)\bar{W}_s$, both \bar{W}_s and \bar{Y}_s increase by Δ .

Let $Q_s = \exp(\alpha \bar{W}_s + \lambda \bar{Y}_s)$ where α and λ are some fixed constants yet to be determined. We will show that Q_s is a supermartingale. Let h be some small time-step. Then

$$\mathbb{E}[Q_{s_0+h} - Q_{s_0} | Q_{s_0}] = h\theta \bar{W}_{s_0} (\exp(\alpha(\bar{W}_{s_0} - 1) + \lambda \bar{Y}_{s_0}) - \exp(\alpha \bar{W}_{s_0} + \lambda \bar{Y}_{s_0})) + \quad (4.47)$$

$$\begin{aligned} & h(1 - \theta) \bar{W}_{s_0} (\exp(\alpha(\bar{W}_{s_0} + \Delta) + \lambda(\bar{Y}_{s_0} + \Delta)) - \exp(\alpha \bar{W}_{s_0} + \lambda \bar{Y}_{s_0})) + \\ & \mathcal{O}(h^2) \\ & = \left(\theta(e^{-\alpha} - 1) + (1 - \theta)(e^{(\alpha+\lambda)\Delta} - 1) \right) h \bar{W}_{s_0} Q_{s_0} + \mathcal{O}(h^2). \end{aligned} \quad (4.48)$$

Dividing through by h and taking h to 0, we have

$$\frac{d}{ds} \mathbb{E}[Q_s | Q_{s_0}] \Big|_{s=s_0} = \left(\theta(e^{-\alpha} - 1) + (1 - \theta)(e^{(\alpha+\lambda)\Delta} - 1) \right) \bar{W}_{s_0} Q_{s_0} \quad (4.49)$$

which is negative for θ sufficiently close to 1. Hence Q_s is a supermartingale for sufficiently large θ .

Define the stopping time

$$\tau = \inf\{s : \bar{W}_s = 0\}. \quad (4.50)$$

Since $(\bar{W}_s, \bar{Y}_s) \geq (W_s, Y_s)$, we have that $W_\tau = 0$ which corresponds to the event that both histories, \mathcal{H}_j and \mathcal{H}_k , have terminated by time τ . Hence

$$\mathbb{P}[\hat{\mathcal{H}}_j \cap \hat{\mathcal{H}}_k \neq \emptyset] \leq \mathbb{P}[Y_\tau \geq |j - k|]. \quad (4.51)$$

Now

$$\mathbb{E}[\exp(\lambda Y_\tau)] \leq \mathbb{E}[\exp(\lambda \bar{Y}_\tau)]. \quad (4.52)$$

and from optional stopping [FIGURE THIS OUT PROPERLY],

$$\mathbb{E}[\exp(\lambda \bar{Y}_\tau)] \leq \mathbb{E}[Q_0] \quad (4.53)$$

$$= \exp(2\alpha). \quad (4.54)$$

Hence

$$\mathbb{P}[Y_\tau \geq |j - k|] \leq \exp(2\alpha) \exp(-\lambda|j - k|) \quad (4.55)$$

and overall we have that

$$\mathbb{P}[\mathcal{H}_j \cap \mathcal{H}_k \neq \emptyset] \leq \exp(2\alpha) \exp(-\lambda|j - k|). \quad (4.56)$$

□

Lemma 4.11.

$$\mathbb{P}[\mathcal{H}_j \cap \mathcal{H}_k \neq \emptyset | X_j = 1] \leq \quad (4.57)$$

Proof. The proof here is similar to that of Lemma 4.10. We first relax to our alternative histories

$$\mathbb{P}[\mathcal{H}_j \cap \mathcal{H}_k \neq \emptyset | X_j = 1] \leq \mathbb{P}[\hat{\mathcal{H}}_j \cap \hat{\mathcal{H}}_k \neq \emptyset | X_j = 1]. \quad (4.58)$$

By symmetry,

$$\mathbb{P}[\hat{\mathcal{H}}_j \cap \hat{\mathcal{H}}_k \neq \emptyset | X_j = 1] = \mathbb{P}[\hat{\mathcal{H}}_j \cap \hat{\mathcal{H}}_k \neq \emptyset | X_k = 1] \quad (4.59)$$

and also

$$\mathbb{P}[X_j = 1] = \mathbb{P}[X_k = 1]. \quad (4.60)$$

So

$$\mathbb{P}[\hat{\mathcal{H}}_j \cap \hat{\mathcal{H}}_k \neq \emptyset | X_j = 1] \leq 2\mathbb{P}[\hat{\mathcal{H}}_j \cap \hat{\mathcal{H}}_k \neq \emptyset | \{X_j = 1\} \cup \{X_k = 1\}]. \quad (4.61)$$

We now define W_s and Y_s as before, except now conditioned on the event $\{X_j = 1\} \cup \{X_k = 1\}$. The effect of this conditioning is to forbid updates that reduce W_s to 0.

HANDWAVING: If we stop when $W_s = 1$ then we can ignore the conditioning???

Define the stopping time

$$\tau = \inf\{s : \bar{W}_s = 1\}. \quad (4.62)$$

□

In [11], Lubetzky and Sly proved something similar...

Lemma 4.12.

$$\mathbb{P}[\mathcal{H}_i(t^* - s) \not\subseteq B(i, l)] \leq \exp(s\Delta^2 - l \ln \Delta) \quad (4.63)$$

Proof. Let $\mathcal{W} = \{\mathbf{w} = (w_1, w_2, \dots, w_l) : w_1 = i, ||w_{k-1} - w_k|| = 1\}$ be the set of length l sequences of adjacent vertices starting at vertex i . If $\mathcal{H}_i(t^* - s) \not\subseteq B(i, l)$ then there must

be some sequence $w \in \mathcal{W}$ such that each w_i was updated at some time $t^* > t_i > t^* - s$ and $t_{k-1} > t_k$. Call this event M_w . For any particular sequence w ,

$$\mathbb{P}[M_w] = \mathbb{P}[\text{Po}(s) \geq l] \quad (4.64)$$

where $\text{Po}(s)$ is Poisson with rate s . By a union bound over \mathcal{W} ,

$$\mathbb{P}[\mathcal{H}_i(t^* - s) \not\subseteq B(i, l)] \leq \Delta^{l-1} \mathbb{P}[\text{Po}(s) \geq l]. \quad (4.65)$$

The moment generating function of a poisson random variable with rate s is

$$M(t) = \exp(s(e^t - 1)). \quad (4.66)$$

Using a Chernoff bound we have for every $t > 0$,

$$\mathbb{P}[\text{Po}(s) \geq l] \leq \exp(s(e^t - 1) - tl). \quad (4.67)$$

Overall we have

$$\mathbb{P}[\mathcal{H}_i(t^* - s) \not\subseteq B(i, l)] \leq \Delta^{l-1} \exp(s(e^t - 1) - tl) \quad (4.68)$$

$$\leq \exp(s(e^t - 1) + l(\ln \Delta - t)). \quad (4.69)$$

Choosing $t = 2 \ln \Delta$,

$$\mathbb{P}[\mathcal{H}_i(t^* - s) \not\subseteq B(i, l)] \leq \exp(s(\Delta^2 - 1) - l \ln \Delta) \quad (4.70)$$

$$\leq \exp(s\Delta^2 - l \ln \Delta) \quad (4.71)$$

$$(4.72)$$

□

Corollary 4.13.

$$\mathbb{P}[\mathcal{H}_i(0) \not\subseteq B(i, l)] \leq \Delta^{-l} n^{\Delta^2} \exp(z\Delta^2) \quad (4.73)$$

For $l \geq \log(n)(\Delta^2 + 1)/\log(\Delta)$

$$\mathbb{P}[\mathcal{H}_i(0) \not\subseteq B(i, l)] \leq \frac{\exp(z\Delta^2)}{n} \quad (4.74)$$

Lemma 4.14. *Blah*

Proof. Write $\bar{\mathcal{H}}_i$ for the history at i but it only has branching updates at rate 1. Write d_j for the time of death of history j . Let $k = |i - j|$.

$$\begin{aligned} \mathbb{P}(\bar{\mathcal{H}}_i \cap \mathcal{H}_j) &= \mathbb{P}(\bar{\mathcal{H}}_i \cap \mathcal{H}_j | d_j < c(k)) \mathbb{P}(d_j < c(k)) \\ &\quad + \mathbb{P}(\bar{\mathcal{H}}_i \cap \mathcal{H}_j | d_j \geq c(k)) \mathbb{P}(d_j \geq c(k)) \end{aligned} \quad (4.75)$$

$$\leq \mathbb{P}(\bar{\mathcal{H}}_i \cap \mathcal{H}_j | d_j < c(k)) + \mathbb{P}(d_j \geq c(k)) \quad (4.76)$$

$$\leq \mathbb{P}(\bar{\mathcal{H}}_i \cap \mathcal{H}_j | d_j < c(k)) + e^{-(1-\beta\Delta)c(k)} \quad (4.77)$$

$$\leq 2\mathbb{P}(\bar{\mathcal{H}}_i(t^* - c(k)) \not\subseteq B(i, k/2)) + e^{-(1-\beta\Delta)c(k)} \quad (4.78)$$

$$\leq \exp(c(k)\Delta^2 - k/2 \ln \Delta) + e^{-(1-\beta\Delta)c(k)} \quad (4.79)$$

$$(4.80)$$

Choosing $c(k) = \ln(k)^2$ works so long as $\beta\Delta < 1$. □

Chapter 5

Conclusion

Part II

Efficient Optimization for Statistical Inference

Chapter 6

Introduction

A gentle introduction to Part [II](#).

Chapter 7

Maximum Likelihood Location Mixtures

7.1 Introduction

7.1.1 Definitions

A location mixture on \mathbb{R} with mixing distribution Q and component density $f(x)$ can be written as

$$f_Q(x) = \int_{-\infty}^{\infty} f(x - \theta) dQ(\theta). \quad (7.1)$$

Given a sample $\mathbf{x} = (x_1, \dots, x_n)$, we wish to find a distribution that maximizes the log likelihood

$$L(Q; \mathbf{x}) = \sum_{i=1}^n \log(f_Q(x_i)). \quad (7.2)$$

Lindsay showed that under quite general conditions, such a maximizing distribution exists and has no more than n points of support [21]. It is therefore common to use

$$f_{\mathbf{p}, \boldsymbol{\theta}}(x) = \sum_{j=1}^m p_j f(x - \theta_j) \quad (7.3)$$

instead of (7.1) as our definition of a location mixture. We note that (7.1) is equivalent to (7.3) in the case where Q is a discrete distribution which places probability masses of weight p_j at locations θ_j , for $j = 1, \dots, m$. The order of the x_i does not matter and so we will assume without loss of generality that $x_1 \leq x_2 \leq \dots \leq x_n$ throughout.

In this paper we are primarily interested in the number of probability masses that are required in the maximizing mixture. We will call this quantity $K_{\mathbf{x}}$. It should be noted

that there is not always a unique mixing distribution that maximizes (7.2). However we can choose $K_{\mathbf{x}}$ to be the smallest number of probability masses that any of the maximizing distributions have.

7.1.2 Flag graphs

One point which we wish to emphasize is that, given a component density f , K is a function of \mathbf{x} only. We can visualise this for small values of n . In Figure 7.1, we empirically found the MLE for $\mathbf{x} = (0, x_2, x_3)$ and recorded the number of probability masses in the maximizing mixture. We took values for x_2 and x_3 from an evenly spaced grid with $-6 \leq x_2, x_3 \leq 6$. We fixed $x_1 = 0$ since the shape of the maximum likelihood mixture (and therefore $K_{\mathbf{x}}$) depends only on the relative location of the x_i , not their absolute location.

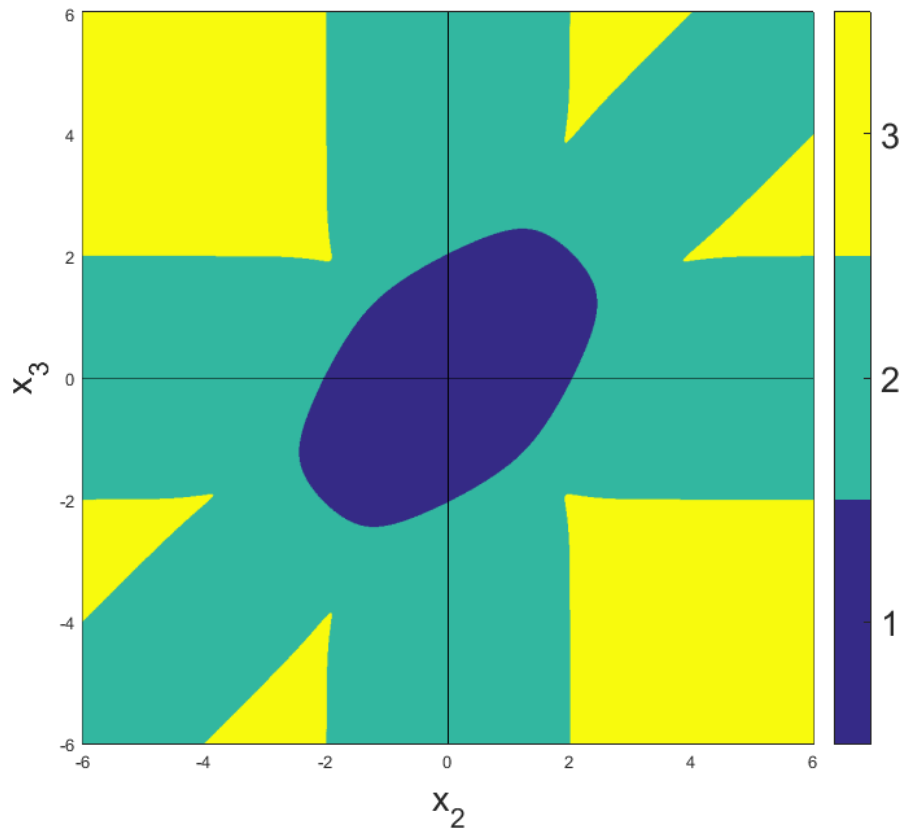


Figure 7.1 – K as a function of x_2 and x_3 (with $x_1 = 0$) for a normal component density with unit variance.

For a particular choice of component density, we can partition \mathbb{R}^n into sets

$$C_k = \{\mathbf{x} \in \mathbb{R}^n | K_{\mathbf{x}} = k\}, \quad k = 1, \dots, n. \quad (7.4)$$

The problem of determining $K_{\mathbf{x}}$ is then the same as determining in which of the C_k \mathbf{x} lies.

7.1.3 Motivating Example

7.2 Results for $n = 2$

In this section, we present Theorem 7.4 which expands upon the results found in [21] and [22].

7.2.1 Things that are referenced

REWORK CONTENTS OF THIS SUBSECTION INTO MAIN TEXT.

$$M(\mathbf{u}) = \sum_{i=1}^n \log(u_i) \quad (7.5)$$

Theorem 7.1. *If Γ is compact then there exists a unique point on the boundary of $\text{Conv}(\Gamma)$ which maximizes the likelihood. This point corresponds to a distribution Q which maximizes the likelihood and that has no more than n point masses.*

7.2.2 The likelihood curve

In [21], the problem of mixture likelihoods was looked at from a geometrical perspective. One key construction introduced by Lindsay was the *likelihood curve*,

$$\gamma(\theta; \mathbf{x}) = (f(x_1 - \theta), \dots, f(x_n - \theta)) \quad (7.6)$$

and its trace,

$$\Gamma_{\mathbf{x}} = \{\gamma(\theta; \mathbf{x}) | \theta \in \mathbb{R}\}. \quad (7.7)$$

A useful property of the likelihood curve is that any convex combination of elements from $\Gamma_{\mathbf{x}}$ can be written as

$$\mathbf{u}(\mathbf{p}, \boldsymbol{\theta}; \mathbf{x}) = (f_{\mathbf{p}, \boldsymbol{\theta}}(x_1), \dots, f_{\mathbf{p}, \boldsymbol{\theta}}(x_n)) = \sum_{j=1}^m p_j \gamma(\theta_j; \mathbf{x}), \quad \sum_{j=1}^m p_j = 1 \quad (7.8)$$

where $f_{\mathbf{p}, \boldsymbol{\theta}}(x)$ is as defined in (7.3). The log likelihood of the corresponding distribution is simply the sum of the log of the components of $\mathbf{u}(\mathbf{p}, \boldsymbol{\theta}; \mathbf{x})$.

One of Lindsay's main results, which follows from this observation, was that if

$$\hat{\mathbf{u}} = \arg \max_{\mathbf{u} \in \text{Conv}(\Gamma_{\mathbf{x}})} \sum_{i=1}^n \log(u_i) \quad (7.9)$$

then we can write

$$\hat{\mathbf{u}} = \mathbf{u}(\mathbf{p}, \boldsymbol{\theta}; \mathbf{x}) \quad (7.10)$$

for some \mathbf{p} and $\boldsymbol{\theta}$ whose dimension is no more than n . Furthermore, the corresponding distribution that places masses p_j at locations θ_j maximizes (7.2). There are some minor conditions on this result, but they will not cause any problems for our purposes and so will not be discussed (see [21] for details).

7.2.2.1 An example

The following example illustrates the geometrical approach given above. We consider the case where $n = 2$. Our sample is made up of two points, $X_1 = 1$ and $X_2 = 2$. We define

$$f_{\theta}(x) = \frac{1}{0.45\sqrt{2\pi}} \exp\left(-\frac{(x - \theta)^2}{2 \cdot 0.45^2}\right) \quad (7.11)$$

(i.e. a normal density with mean θ and variance $\sigma^2 = 0.45^2$) to be our component density. We trace out the set Γ in Figure 7.2.

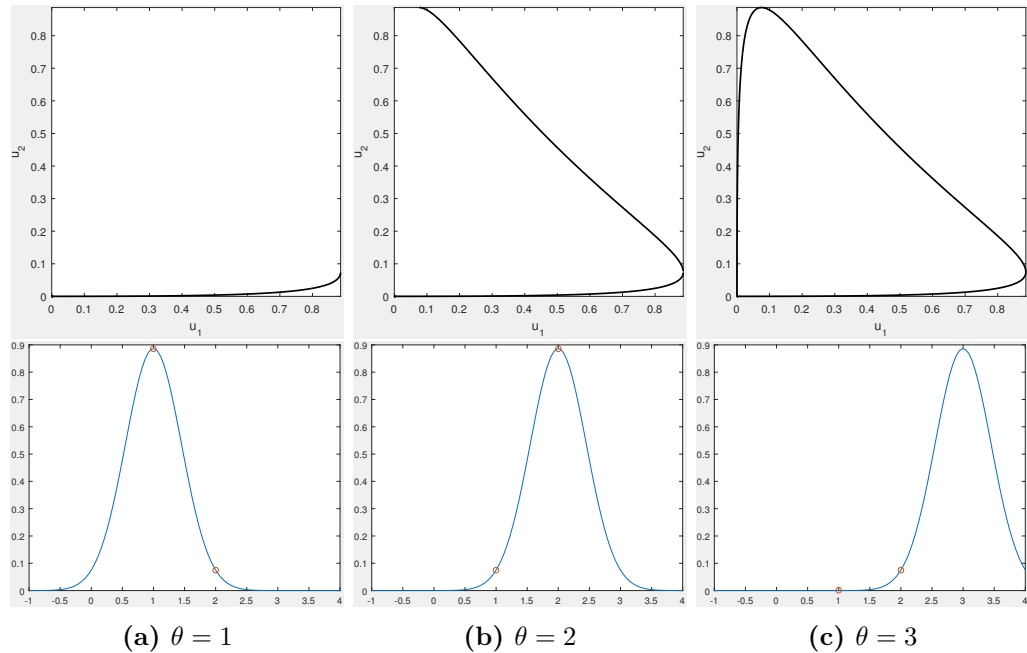


Figure 7.2 – The blue density is f_{θ} for $\theta = 1, 2, 3$. Each value of θ contributes a point to Γ whose coordinates are given by $(f_{\theta}(X_1), f_{\theta}(X_2))$ (represented by the red circles). As we increase θ from $-\infty$ to ∞ we trace out more of Γ (shown above).

Note that while Γ is bounded, it is not closed (it does not contain the limit point $(0, 0)$), and so Γ is not compact (as required by Theorem 7.1). In fact, any positive density whose support is the whole real line will not contain the limit point $\mathbf{0}$ (where $\mathbf{0}$ represents the zero vector in \mathbb{R}^n). However, since $\mathbf{0}$ is clearly not going to be a part of a maximizing mixture, we are safe to apply Theorem 7.1 if $\Gamma \cup \{\mathbf{0}\}$ is compact.

We trace the boundary of $\text{Conv}(\Gamma)$ in Figure 7.3 along with a heat map of the objective function (7.5). The optimal point is on the boundary of $\text{Conv}(\Gamma)$ as expected and it can

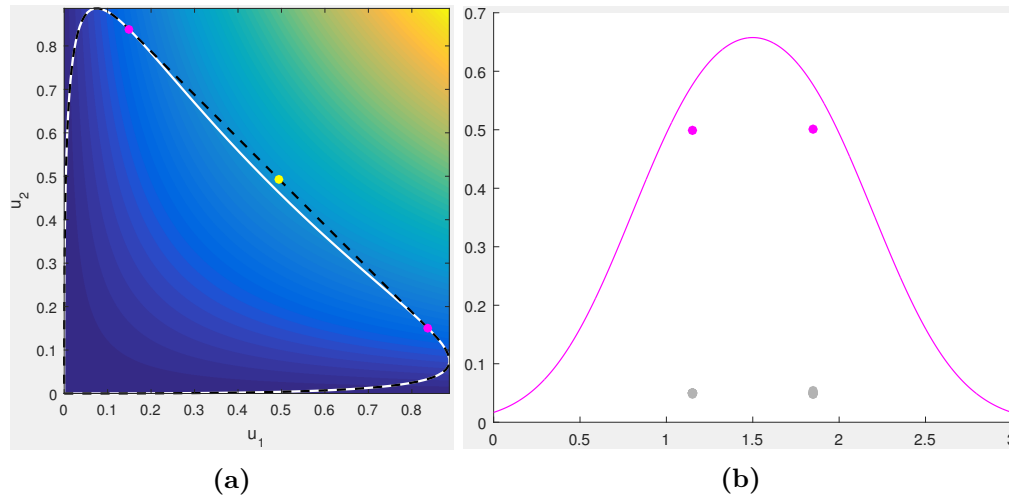


Figure 7.3 – In (a), the boundary of $\text{Conv}(\Gamma)$ is shown as a dashed black line, Γ is the white curve, the heat map shows the objective function (likelihood increases from blue to yellow) and the yellow point is the maximizing point which can be written as the convex combination of the two magenta points. These two magenta points correspond to the two probability masses in the maximizing mixing distribution (b).

be written as the $p_1 \mathbf{f}(\theta_1) + p_2 \mathbf{f}(\theta_2)$ (where $p_1 + p_2 = 1$). These two points correspond to the two probability masses in the maximizing mixture distribution shown in Figure 7.3b. These masses are located at θ_1 and θ_2 with weights p_1 and p_2 .

7.2.3 The likelihood curve for $n = 2$

The shape of $\Gamma_{\mathbf{x}}$ can provide us with some insight into the behaviour of $K_{\mathbf{x}}$. In Figure 7.4, we give some examples of $\Gamma_{\mathbf{x}}$ for $n = 2$ using a normal component density with variance $\sigma^2 = 1$. In particular, we note that the distance between x_1 and x_2 has a strong effect on the shape of $\Gamma_{\mathbf{x}}$. In Figure 7.4a, the points are distance 1 apart and $\Gamma_{\mathbf{x}}$ is the boundary of $\text{Conv}(\Gamma_{\mathbf{x}})$. In this case, it is clear that $K_{\mathbf{x}} = 1$. In Figure 7.4c, the points are distance 3 apart and the optimal point no longer lies on $\Gamma_{\mathbf{x}}$. This results in the maximum likelihood mixing distribution needing two points of support and so $K_{\mathbf{x}} = 2$. The boundary case, where $\Gamma_{\mathbf{x}}$ goes from being a convex curve to having the indentation shown in Figure 7.4b, is shown in Figure 7.4b.

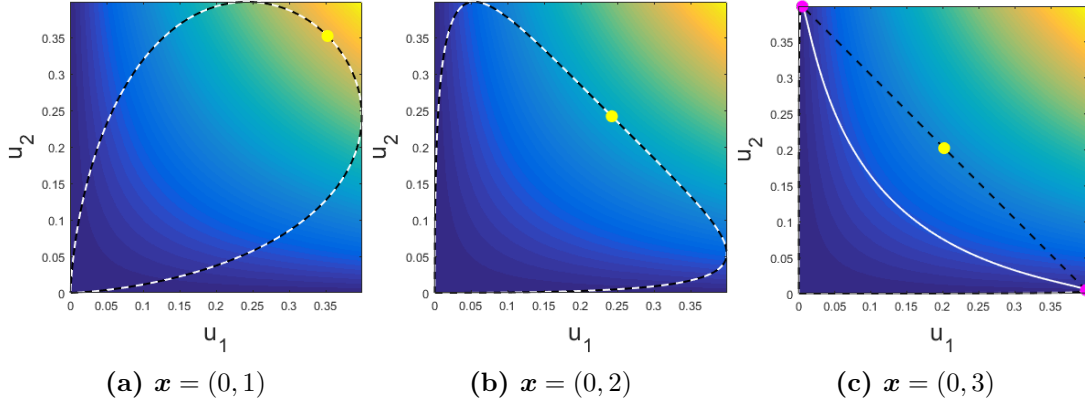


Figure 7.4 – The curve Γ_x for three different x along with the boundary of $\text{Conv}(\Gamma_x)$. The objective function from (7.9) is represented as a heat map. The optimal point $\hat{\mathbf{u}}$ is shown in yellow, and where applicable, the points $\gamma(\theta_j)$ that make up $\hat{\mathbf{u}}$ (as in (7.8)) are shown in magenta.

Obtaining results about where these boundaries lie is very difficult in higher dimensions. In [22], Lindsay used the sign of the curvature of $\gamma(\theta; x)$ to obtain results for $n = 2$ when the component density is in the exponential family. Here we will present an extension to Lindsay’s results by considering densities that satisfy the following assumptions.

A1 (Continuity). $f(x)$ is a continuous density and has the whole real line as its support.

A2 (Differentiability). $f(x)$ is twice differentiable.

A3 (Unimodality). $f(x)$ has a single mode at $x = 0$. I.e. $f'(x) > 0$ for $x < 0$, $f'(0) = 0$, and $f'(x) < 0$ for $x > 0$.

A4 (Symmetry). The density $f(x)$ is symmetric about $x = 0$.

A5. f has only two points of inflection

Definition 7.2. If f satisfies assumptions A1 through to A3, then define $[i^-, i^+]$ to be the largest interval that contains 0 and on which $f''(x) \leq 0$.

That is, i^- and i^+ are inflection points of f . Note that for any f satisfying A4, $i^- = -i^+$. In this case we will write $i = i^+ = -i^-$.

A6. $f'(x) > -f'(x - 2i)$ for $\theta \in (i, \infty)$

Some common densities that satisfy these assumptions include the normal density and the Cauchy density.

Lemma 7.3. Let $f(x)$ be a density which satisfies assumptions A1 through to A6 and whose inflection points are at $x = i$ and $x = -i$. If $x_2 - x_1 < 2i$ ($x_2 > x_1$) then the equation

$$-f'(x_1 - \theta) = f'(x_2 - \theta) \quad (7.12)$$

has only one solution.

Proof. We first consider the shape of $f'(x)$. Assumption A3 tells us that $f'(x)$ is positive for $x < 0$ and negative for $x > 0$. The function $f'(x)$ will have turning points at $\pm i$ and from Assumption A5 these will be the only turning points. Hence we have the following picture of $f'(x)$:

$$f'(x) \text{ is } \begin{cases} \text{positive and increasing,} & x \in (-\infty, -i) \\ \text{positive and decreasing,} & x \in (-i, 0) \\ \text{negative and decreasing,} & x \in (0, i) \\ \text{negative and increasing,} & x \in (i, \infty). \end{cases} \quad (7.13)$$

We also note, from A4, that $f'(x)$ is an odd function. Using this and rearranging (7.12) we obtain the equivalent equation

$$g(\theta) = h(\theta) \quad (7.14)$$

where we have put $g(\theta) = f'(\theta)$ and $h(\theta) = -f'(\theta - (x_2 - x_1))$ for ease of notation.

If we assume that $0 < x_2 - x_1 < 2i$ then we can consider possible solutions to (7.14) on each of the following intervals.

For $\theta \in (-\infty, 0]$, $g(\theta) \geq 0$ and $h(\theta) < 0$ and so there are no possible solutions.

Likewise, for $\theta \in [x_2 - x_1, \infty)$, $g(\theta) < 0$ and $h(\theta) \geq 0$ and so there are no possible solutions.

For $\theta \in [-i + x_2 - x_1, i]$, $g(\theta)$ is decreasing and $h(\theta)$ is increasing and $h(-i + x_2 - x_1) = g(i)$ (since f' is odd). Therefore there must be exactly one solution in this interval.

We note that if $x_2 - x_1 \leq i$ then the above intervals cover the real line. In the case that $i < x_2 - x_1 < 2i$ we need to consider these additional intervals.

For $\theta \in (i, x_2 - x_1)$, from assumption A6, $f'(\theta) < -f'(\theta - 2i) < -f'(\theta - (x_2 - x_1))$ since both $-f'(\theta - 2i)$ and $-f'(\theta - (x_2 - x_1))$ are increasing on this interval. Hence there can be no solutions to (7.14) on this interval.

Similarly by symmetry of f , for $\theta \in (0, -i + x_2 - x_1)$, $f'(\theta) > -f'(\theta - 2i) > -f'(\theta - x_2 - x_1)$ and there are no solutions to (7.14) on this interval either.

Since the above intervals cover the real line and since we have shown that there is only one solution in one of these intervals, (7.12) must have only one solution. \square

Theorem 7.4. *Let $f(x)$ satisfy assumptions A1 through to A6. Let $\mathbf{x} = (x_1, x_2)$ be the sample for which we are finding a maximum likelihood mixture using f as the component density. Then $K_{\mathbf{x}} = 1$ if and only if*

$$x_2 - x_1 \leq 2i \quad (7.15)$$

Proof. By the unimodality of f , the points of support of the maximizing mixing distribution must lie between x_1 and x_2 . Hence we need only consider the behaviour of $\gamma(\theta; \mathbf{x})$ for $\theta \in [x_1, x_2]$. By the symmetry of f , $\hat{\mathbf{u}}$ must lie on the line $u_1 = u_2$ ¹.

First we complete the only if direction of the proof. Assume that $x_2 - x_1 > 2i$. By the symmetry of f , $\gamma(\theta; \mathbf{x})$ crosses the $u_1 = u_2$ line at $\theta = (x_1 + x_2)/2$. Now the curvature of γ has sign equal to

$$S(\theta) = \begin{vmatrix} \gamma'_1(\theta; \mathbf{x}) & \gamma''_1(\theta; \mathbf{x}) \\ \gamma'_2(\theta; \mathbf{x}) & \gamma''_2(\theta; \mathbf{x}) \end{vmatrix} = \begin{vmatrix} -f'(x_1 - \theta) & f''(x_1 - \theta) \\ -f'(x_2 - \theta) & f''(x_2 - \theta) \end{vmatrix}. \quad (7.16)$$

and so

$$S\left(\frac{x_1 + x_2}{2}\right) = \begin{vmatrix} -f'\left(\frac{x_1 - x_2}{2}\right) & f''\left(\frac{x_1 - x_2}{2}\right) \\ -f'\left(\frac{x_2 - x_1}{2}\right) & f''\left(\frac{x_2 - x_1}{2}\right) \end{vmatrix}. \quad (7.17)$$

Since $x_2 - x_1 > 2i$, $\frac{x_1 - x_2}{2} > i$ and so $f''((x_1 - x_2)/2) > 0$. Similarly, $f''((x_2 - x_1)/2) > 0$. We also have that $-f'((x_1 - x_2)/2) < 0$ and $-f'((x_2 - x_1)/2) > 0$. Hence $S((x_1 + x_2)/2) < 0$ and so $\gamma((x_1 + x_2)/2; \mathbf{x})$ has negative curvature. The curve Γ must have positive curvature at the points of support and so we cannot have that $K_{\mathbf{x}} = 1$.

Now we complete the if direction. Assume that $x_2 - x_1 \leq 2i$. By Lemma 7.3, there is only one point at which the curve is pointing perpendicular to the line $u_1 = u_2$ SAY THIS BETTER. By the symmetry of f this occurs when $\gamma(\theta; \mathbf{x})$ is crossing the line $u_1 = u_2$. Since f is continuous, the direction that $\gamma(\theta; \mathbf{x})$ is moving is also continuous. At $\theta = x_1$, $\gamma(\theta; \mathbf{x})$ is pointing straight up and so we have that for $\theta \in [x_1, (x_1 + x_2)/2]$, $\gamma(\theta; \mathbf{x})$ is travelling in a direction pointing above the line perpendicular to $u_1 = u_2$. For $\theta \in [(x_1 + x_2)/2, x_2]$, $\gamma(\theta; \mathbf{x})$ points below the line. It is now obvious that $\gamma((x_1 + x_2)/2; \mathbf{x})$ is the furthest point from the origin that lies on $u_1 = u_2$ and is in the convex hull of $\Gamma_{\mathbf{x}}$. Since the likelihood increases as we move away from the origin along the line $u_1 = u_2$ in the positive quadrant, we must have

$$\hat{\mathbf{u}} = \gamma((x_1 + x_2)/2; \mathbf{x})$$

and so $K_{\mathbf{x}} = 1$.

¹This is obvious but may need a lemma

□

7.3 Results for general n

7.3.1 Directional Derivative

One of the tools introduced in [21] was the function

$$D(\theta; \mathbf{p}, \boldsymbol{\theta}, \mathbf{x}) = -n + \sum_{i=1}^n \frac{f(x_i - \theta)}{\sum_{j=1}^m p_j f(x_i - \theta_j)}. \quad (7.18)$$

Lindsay showed that if $\hat{\boldsymbol{\theta}}$ and $\hat{\mathbf{p}}$ form a maximum likelihood location mixture of f for \mathbf{x} then (under appropriate differentiability assumptions) the function D satisfies the following:

$$D(\theta_k; \hat{\mathbf{p}}, \hat{\boldsymbol{\theta}}, \mathbf{x}) = 0, \quad k = 1, \dots, m, \quad (7.19)$$

$$D'(\theta_k; \hat{\mathbf{p}}, \hat{\boldsymbol{\theta}}, \mathbf{x}) = 0, \quad k = 1, \dots, m, \quad (7.20)$$

$$D''(\theta_k; \hat{\mathbf{p}}, \hat{\boldsymbol{\theta}}, \mathbf{x}) \leq 0, \quad k = 1, \dots, m. \quad (7.21)$$

These three constraints restrict what a potential maximum likelihood solution can look like. HOW DID LINDSAY USE THEM VS US?

7.3.2 Normal Constraints

When our component density is normal with variance σ^2 ,

$$f(x; \sigma) = \frac{1}{\sigma\sqrt{2\pi}} e^{-x^2/2\sigma^2}, \quad (7.22)$$

equations (7.19) to (7.21) become

$$\frac{1}{n} \sum_{i=1}^n \Gamma_k(x_i; \mathbf{p}, \boldsymbol{\theta}) = 1 \quad (7.23)$$

$$\frac{1}{n} \sum_{i=1}^n x_i \Gamma_k(x_i; \mathbf{p}, \boldsymbol{\theta}) = \theta_k \quad (7.24)$$

$$\frac{1}{n} \sum_{i=1}^n (x_i - \theta_k)^2 \Gamma_k(x_i; \mathbf{p}, \boldsymbol{\theta}) \leq \sigma^2 \quad (7.25)$$

where we have written

$$\Gamma_k(x; \mathbf{p}, \boldsymbol{\theta}) = \frac{f(x - \theta_k; \sigma)}{\sum_{j=1}^m p_j f(x - \theta_j; \sigma)}. \quad (7.26)$$

for ease of notation. Using these constraints, we will bound the regions C_1, \dots, C_n in Theorem 7.10. However, as a gentle introduction we will start with the much simpler problem of just bounding C_1 .

Theorem 7.5. *Write $\bar{\mathbf{x}}$ for the mean of \mathbf{x} . If $\mathbf{x} \in C_1$ then*

$$\frac{1}{n} \sum_{i=1}^n (x_i - \bar{\mathbf{x}})^2 \leq \sigma^2. \quad (7.27)$$

Proof. If $\mathbf{x} \in C_1$ then the maximizing mixture has one component and so $\Gamma_1(x; \boldsymbol{\theta}, \mathbf{p}) = 1$. Then (7.24) gives us that $\theta_1 = \bar{\mathbf{x}}$ and combining this with (7.25) completes the proof. \square

7.3.2.1 Treating \mathbf{x} as random

Up until now, we have treated \mathbf{x} as fixed, not random, and treated the maximum likelihood problem purely as an optimization one, rather than a statistical one. However, for this section we make the assumption that \mathbf{x} is made up of i.i.d. random variables, x_i , which have distribution

$$x_i \sim N(\mu, \sigma_1^2)$$

for $i = 1, \dots, n$. Our component density, f_θ , is normal with variance σ_2^2 . From Theorem 7.5,

$$p_u = \mathbb{P} \left(\sum_{i=1}^n (x_i - \bar{\mathbf{x}})^2 \leq n\sigma_2^2 \right)$$

is an upper bound to $\mathbb{P}(\mathbf{x} \in C_1)$. Writing s^2 for the unbiased sample variance of \mathbf{x}

$$\begin{aligned} p_u &= \mathbb{P} \left(s^2 \leq \frac{n\sigma_2^2}{n-1} \right) \\ &= \mathbb{P} \left(\frac{(n-1)s^2}{\sigma_1^2} \leq \frac{n\sigma_2^2}{\sigma_1^2} \right) \\ &= \mathbb{P} \left(\chi_{n-1}^2 \leq \frac{n\sigma_2^2}{\sigma_1^2} \right) \end{aligned}$$

where χ_{n-1}^2 is chi-squared with $n-1$ degrees of freedom.

Remark 7.6. Of particular interest is the case where $\sigma_1 = \sigma_2$. In this case, $p_u \rightarrow 1/2$ as $n \rightarrow \infty$. While not a new result [CITE SOMETHING HERE], this tells us

that the maximum likelihood estimator is not a consistent estimator for the number of components.

7.3.3 Properties of Γ

In order to bound regions where $m \geq 2$, we will need to get a handle on $\Gamma_k(x; \boldsymbol{\theta}, \mathbf{p})$. In this section, we list and prove some properties that will be required in Section 7.3.4.

Lemma 7.7.

$$\max_k (\Gamma_k(x; \mathbf{p}, \boldsymbol{\theta})) \geq 1 \quad (7.28)$$

Proof. For each x , there exists a k_0 such that $f(x - \theta_{k_0}; \sigma) \geq f(x - \theta_k; \sigma)$ for all k . It follows that

$$\Gamma_{k_0}(x; \mathbf{p}, \boldsymbol{\theta}) = \frac{f(x - \theta_{k_0}; \sigma)}{\sum_{j=1}^m p_j f(x - \theta_j; \sigma)} \geq \frac{f(x - \theta_{k_0}; \sigma)}{\sum_{j=1}^m p_j f(x - \theta_{k_0}; \sigma)} = 1. \quad (7.29)$$

□

Lemma 7.8.

$$\Gamma_k(x; \mathbf{p}, \boldsymbol{\theta}) \leq \frac{1}{p_k} \quad (7.30)$$

Proof. Since $f(x) > 0$,

$$\Gamma_k(x; \mathbf{p}, \boldsymbol{\theta}) = \frac{f(x - \theta_k; \sigma)}{\sum_{j=1}^m p_j f(x - \theta_j; \sigma)} \leq \frac{f(x - \theta_k; \sigma)}{p_k f(x - \theta_k; \sigma)} = \frac{1}{p_k}. \quad (7.31)$$

□

Lemma 7.9. Let $\gamma(x)$ be a non-negative function that satisfies

$$\frac{1}{n} \sum_{i=1}^n \gamma(x_i) = 1. \quad (7.32)$$

Then the θ that minimizes

$$\frac{1}{n} \sum_{i=1}^n (x_i - \theta)^2 \gamma(x_i) \quad (7.33)$$

is

$$\theta = \frac{1}{n} \sum_{i=1}^n x_i \gamma(x_i). \quad (7.34)$$

Proof. CURRENTLY UNUSED. PROOF IN TIM'S NOTEBOOK. □

7.3.4 Bounding C_m

Theorem 7.10. *THM AND PROOF IS BELOW*

Let $\mathbf{x} = (x_1, \dots, x_n)$ and assume that the maximum likelihood mixture for \mathbf{x} has no more than m components. Let $\hat{\boldsymbol{\theta}}$ and $\hat{\mathbf{p}}$ denote this maximizing mixture. Then by Lemma 7.7, there exists a k^* such that $\Gamma_{k^*}(x_i; \hat{\mathbf{p}}, \hat{\boldsymbol{\theta}}) \geq 1$ for at least $\lceil \frac{n}{m} \rceil$ different x_i . Let A_{k^*} be the set of all these x_i . Let $A_{\theta_{k^*}}$ be the set of the $|A_{k^*}|$ closest x_i to θ_{k^*} . Then

$$\frac{1}{n} \sum_{i=1}^n (x_i - \theta_{k^*})^2 \Gamma_{k^*}(x_i; \hat{\mathbf{p}}, \hat{\boldsymbol{\theta}}) \geq \frac{1}{n} \sum_{i \in A_{\theta_{k^*}}} (x_i - \theta_{k^*})^2 \quad (7.35)$$

$$\geq \frac{1}{n} \left\lceil \frac{n}{m} \right\rceil \text{Var}(A_{\theta_{k^*}}) \quad (\text{Biased Variance}) \quad (7.36)$$

From (7.25),

$$\text{Var}(A_{\theta_{k^*}}) \leq \frac{n\sigma^2}{\left\lceil \frac{n}{m} \right\rceil}. \quad (7.37)$$

This means that if we cannot find a subset of the x_i that has at least $\frac{n}{m}$ elements and has (biased) variance less than $\frac{n\sigma^2}{\left\lceil \frac{n}{m} \right\rceil}$ then we need more than m components in our maximum likelihood mixture.

7.3.5 A particular class of optimization problem

”The results follow from this general theorem which seems obvious.”

Theorem 7.11. *Let $(E_m)_{m=1}^\infty$ be a sequence of appropriately defined sets and let $(g_m)_{m=1}^\infty, g_m : E_m \mapsto \mathbb{R}$ be a sequence of functions that satisfy the following properties*

1. $\forall \mathbf{x} \in \partial E_m, \exists n < m, \mathbf{y} \in E_n$ such that $g_m(\mathbf{x}) \leq g_n(\mathbf{y})$.
2. $\exists m_0, \mathbf{x}_0 \in E_{m_0}$ such that $\forall m, \mathbf{x} \in E_m, g_m(\mathbf{x}) \leq g_{m_0}(\mathbf{x}_0)$.

Then $\exists m_, \mathbf{x}_* \in E_{m_*} \setminus \partial E_{m_*}$ such that $\forall m, \mathbf{x} \in E_m, g_m(\mathbf{x}) \leq g_{m_*}(\mathbf{x}_*)$.*

Proof. The proof is simple. If $\mathbf{x}_0 \notin \partial E_{m_0}$ then we are done. Otherwise, by property 1 we can find a n and $\mathbf{y} \in E_n$ such that $g_n(\mathbf{y}) = g_{m_0}(\mathbf{x}_0)$. If $\mathbf{y} \notin \partial E_n$ then we are done, otherwise we repeat the process until we find a m, \mathbf{x} pair with $\mathbf{x} \notin \partial E_m$. \square

7.3.6 Derive Constraints again

WE SHOULD BE ABLE TO DERIVE (7.23) THROUGH (7.25) AGAIN USING THEOREM 7.11.

7.4 General Results

7.4.1 All points separated by α

Consider the situation in which $|x_i - x_j| > \alpha$ for all $i \neq j$. Intuitively, we would expect that there is some α^* such that if $\alpha > \alpha^*$ then $\mathbf{x} \in C_n$.

Theorem 7.12. *If our component density is unimodal and symmetric about zero, and*

$$\frac{f(\alpha/2)}{f(0)} < \frac{1}{n} \left(\frac{n-1}{n} \right)^{n-1}.$$

Then if $|x_i - x_j| > \alpha$ for all $i \neq j$, $\mathbf{x} \in C_n$.

Proof. Let \hat{f}_{n-1} be the maximum likelihood mixture density of \mathbf{x} with no more than $n-1$ components and let L_{n-1} be the corresponding likelihood. Since all the x_i are separated by at least α , there exists an x_{i^*} such that $|x_{i^*} - \theta_j| > \frac{\alpha}{2}$ for all j . Hence

$$\hat{f}_{n-1}(x_{i^*}) < f(\alpha/2)$$

and so

$$L_{n-1} < f(\alpha/2) \prod_{i \neq i^*} \hat{f}_{n-1}(x_i).$$

We will now construct a mixture density that has one more component than \hat{f}_{n-1} . We do this by scaling all the components of \hat{f}_{n-1} by a factor of $\frac{n-1}{n}$ and introducing a new component with parameters $(p, \theta) = (\frac{1}{n}, x_{i^*})$. Call this function f_n^* and the corresponding likelihood L_n . Now

$$L_n > \frac{f(0)}{n} \left(\frac{n-1}{n} \right)^{n-1} \prod_{i \neq i^*} \hat{f}_{n-1}(x_i).$$

So if $f(\alpha/2) < \frac{f(0)}{n} \left(\frac{n-1}{n} \right)^{n-1}$ then $L_n > L_{n-1}$ and so $\mathbf{x} \in C_n$. □

7.4.2 Discussion about what we hope to achieve

The few original results above (Theorems 7.4 and 7.10) seem to be special cases of what looks to be a much more general rule. Theorem 7.10 seems to be too large by a factor of m when you compare to numerics, and the distance between inflection points in Theorem 7.4 seems to come up again when you look at images like Figure 7.1 (eg the thickness of the ‘bands’ is this distance). It is therefore our hope that we can either generalize or add significantly to the Theorems stated so far.

Chapter 8

Deconvolution

8.1 Introduction

From here to the end of Section 8.1.2 is a summary of [23]. We want to find the distribution of a random variable X but only measure

$$W = X + U$$

where U is symmetric (and hence $\phi_U(t)$ is real-valued and even). We also additionally require that $\phi_U(t) \geq 0$. We write

$$\rho_X = \frac{\phi_X}{|\phi_X|}$$

for the phase function of X . Then

$$\begin{aligned} \phi_W &= \phi_X \phi_U && \text{as } X \text{ and } U \text{ are independent,} \\ \frac{\phi_W}{|\phi_W|} &= \frac{\phi_X}{|\phi_X|} \frac{\phi_U}{|\phi_U|}, \\ \rho_W &= \rho_X && \text{as } \phi_U \text{ is real and non-negative.} \end{aligned}$$

Given a probability distribution, there are an infinite number of other distributions that have the same phase function. We make the choice that out of all the distributions with phase function ρ_W , we choose the one that has smallest variance. Hence, we want to find a distribution F_Y that minimizes $\text{Var}(Y)$ such that

$$\rho_Y = \rho_W.$$

8.1.1 Optimization problem

Ideally, we would like to minimize the variance of Y under the constraint that $\rho_Y = \rho_W$. However, we can't do this since we only estimate $\rho_W(t)$ from a random sample of size n and this estimate is bad for large $|t|$. So we instead choose a Y_0 to minimize

$$T(Y) = \int_{-\infty}^{\infty} \left| \hat{\phi}_W(t) - |\hat{\phi}_W(t)|\rho_Y(t) \right|^2 w(t) dt \quad (8.1)$$

where $w(t)$ is some suitably chosen weight function and $\hat{\phi}_W(t)$ is our empirical estimate for $\phi_W(t)$. We then search for Y which minimizes $\text{Var}(Y)$ subject to $T(Y) \leq T(Y_0)$.

We restrict our search to Y discrete with point masses p_j at locations x_j for $j = 1, 2, \dots, m$. We place our x_j uniformly at random along the interval $[\min W, \max W]$ and choose the p_j to solve the optimization problem described above. Numerical investigations indicate that $m = 5\sqrt{n}$ is a reasonable choice.

8.1.2 Kernel Smoothing

Once we have our discrete distribution Y we can create a continuous density approximation using

$$\hat{f}_Y(x) = \frac{1}{2\pi} \int e^{-itx} \phi_Y(t) \phi_K(ht) dt \quad (8.2)$$

where K is some kernel with bandwidth h . This is exactly equivalent to

$$\hat{f}_Y(x) = \sum_{j=1}^m p_j K_h(x - x_j). \quad (8.3)$$

However, we can get a better result by using (8.2) and replacing $\phi_Y(t)$ with an appropriate ridge function for $t \geq t^*$.

8.2 Examples and Relation to Mixture Phenomenon

8.3 R Package

Bibliography

- [1] Ernst Ising. Beitrag zur theorie des ferromagnetismus. *Zeitschrift für Physik*, 31 (1):253–258, February 1925.
- [2] Wilhelm Lenz. Beiträge zum verständnis der magnetischen eigenschaften in festen körpern. *Phys. Z.*, 21:613–615, 1920.
- [3] Sacha Friedli and Yvan Velenik. *Statistical Mechanics of Lattice Systems: A Concrete Mathematical Introduction*. Cambridge University Press, November 2017.
- [4] R Peierls. On ising’s model of ferromagnetism. *Math. Proc. Cambridge Philos. Soc.*, 32(3):477–481, October 1936.
- [5] Lars Onsager. Crystal statistics. i. a Two-Dimensional model with an Order-Disorder transition. *Phys. Rev.*, 65(3-4):117–149, February 1944.
- [6] Mark Jerrum and Alistair Sinclair. Polynomial-time approximation algorithms for the ising model. *SIAM J. Comput.*, 22(5):1087–1116, 1993.
- [7] James Gary Propp and David Bruce Wilson. Exact sampling with coupled markov chains and applications to statistical mechanics. 1996.
- [8] David A Levin, Yuval Peres, and Elizabeth L Wilmer. *Markov chains and mixing times*. American Mathematical Society, 2009.
- [9] Olle Häggström. *Finite Markov Chains and Algorithmic Applications*. Cambridge University Press, May 2002.
- [10] Mark Jerrum. Mathematical foundations of the markov chain monte carlo method. In Michel Habib, Colin McDiarmid, Jorge Ramirez-Alfonsin, and Bruce Reed, editors, *Probabilistic Methods for Algorithmic Discrete Mathematics*, pages 116–165. Springer Berlin Heidelberg, Berlin, Heidelberg, 1998.
- [11] Eyal Lubetzky and Allan Sly. Information percolation and cutoff for the stochastic ising model. *J. Amer. Math. Soc.*, 2016.

-
- [12] P Diaconis. The cutoff phenomenon in finite markov chains. *Proc. Natl. Acad. Sci. U. S. A.*, 93(4):1659–1664, February 1996.
 - [13] David Aldous. Random walks on finite groups and rapidly mixing markov chains. In *Séminaire de Probabilités XVII 1981/82*, pages 243–297. Springer Berlin Heidelberg, 1983.
 - [14] Eyal Lubetzky and Allan Sly. Cutoff for the ising model on the lattice. *Invent. Math.*, 191(3):719–755, March 2013.
 - [15] Eyal Lubetzky and Allan Sly. Universality of cutoff for the ising model. *Ann. Probab.*, 45(6A):3664–3696, November 2017.
 - [16] Danny Nam and Allan Sly. Cutoff for the Swendsen-Wang dynamics on the lattice. May 2018.
 - [17] Andrea Collecchio, Eren Metin Elci, Timothy M Garoni, and Martin Weigel. On the coupling time of the heat-bath process for the Fortuin-Kasteleyn random-cluster model. May 2017.
 - [18] A D Barbour and O Chrysaphinou. Compound poisson approximation: a user’s guide. *Ann. Appl. Probab.*, 11(3):964–1002, August 2001.
 - [19] A D Barbour, Louis H. Y. Chen, and Wei-Liem Loh. Compound poisson approximation for nonnegative random variables via stein’s method. *Ann. Probab.*, 20(4):1843–1866, 1992.
 - [20] Eyal Lubetzky and Allan Sly. An exposition to information percolation for the ising model. December 2014.
 - [21] Bruce G Lindsay. The geometry of mixture likelihoods: A general theory. *Ann. Stat.*, 11(1):86–94, March 1983.
 - [22] Bruce G Lindsay. The geometry of mixture likelihoods, part II: The exponential family. *Ann Stat*, 11(3):783–792, September 1983.
 - [23] Aurore Delaigle and Peter Hall. Methodology for non-parametric deconvolution when the error distribution is unknown. *Journal of the Royal Statistical Society: Series B (Statistical Methodology)*, 78(1):231–252, January 2016.